SYNTHESIS, CHARACTERIZATION AND ENCAPSULATION STUDIES OF MIXED DIORGANOTIN DITHIOCARBAMATES COMPLEXES

NORDIYANA BINTI ZALDI

FACULTY OF SCIENCE
UNIVERSITY OF MALAYA
KUALA LUMPUR

2018

SYNTHESIS, CHARACTERIZATION AND ENCAPSULATION STUDIES OF MIXED DIORGANOTIN DITHIOCARBAMATES COMPLEXES

NORDIYANA BINTI ZALDI

THESIS SUBMITTED IN FULFILMENT OF THE REQUIREMENTS FOR THE DEGREE OF MASTER OF SCIENCE

DEPARTMENT OF CHEMISTRY
FACULTY OF SCIENCE
UNIVERSITY OF MALAYA
KUALA LUMPUR

2018

UNIVERSITY OF MALAYA

ORIGINAL LITERARY WORK DECLARATION

Name of Candidate: NORDIYANA BINTI ZALDI

Matric No: SGR150062

Name of Degree: MASTER

Title of Project Paper/Research Report/Dissertation/Thesis ("this Work"):

SYNTHESIS, CHARACTERIZATION AND ENCAPSULATION STUDIES OF MIXED DIORGANOTIN DITHIOCARBAMATES COMPLEXES

Field of Study: INORGANIC CHEMISTRY

I do solemnly and sincerely declare that:

(1) I am the sole author/writer of this Work;
(2) This Work is original;
(3) Any use of any work in which copyright exists was done by way of fair dealing and for permitted purposes and any excerpt or extract from, or reference to or reproduction of any copyright work has been disclosed expressly and sufficiently and the title of the Work and its authorship have been acknowledged in this Work;
(4) I do not have any actual knowledge nor do I ought reasonably to know that the making of this work constitutes an infringement of any copyright work;
(5) I hereby assign all and every rights in the copyright to this Work to the University of Malaya ("UM"), who henceforth shall be owner of the copyright in this Work and that any reproduction or use in any form or by any means whatsoever is prohibited without the written consent of UM having been first had and obtained;
(6) I am fully aware that if in the course of making this Work I have infringed any copyright whether intentionally or otherwise, I may be subject to legal action or any other action as may be determined by UM.

Candidate's Signature Date:

Subscribed and solemnly declared before,

Witness's Signature Date:

Name:

Designation:

SYNTHESIS, CHARACTERIZATION AND ENCAPSULATION STUDIES OF MIXED DIORGANOTIN DITHIOCARBAMATE COMPLEXES

ABSTRACT

Organotin and dithiocarbamate compounds are well-known anticancer agents and exhibit cytotoxic activities such as antiproliferative and antitumour. This research focused on the synthesis, characterization, and formulation studies of diorganotin(IV) dithiocarbamate complexes to identify their potential on anticancer properties. A total of ten mixed diorganotin(IV) dithiocarbamates complexes were successfully synthesized by the reaction of dithiocarbamate ligand with dimethyltin(IV) dichloride. The complexes were characterized by Fourier Transform Infrared (FT-IR), Nuclear Magnetic Resonance (NMR), and Ultraviolet-visible (UV-Vis) absorption spectroscopy as well as Carbon, Hydrogen, Nitrogen, and Sulphur (CHNS) elemental analysis. The molecular structure of dimethyltin(IV) *bis*(morpholinodithiocarbamate) was determined by X-ray crystallography, showing a skew-trapezoidal bipyramidal coordination geometry. The dithiocarbamate ligands and its corresponding organotin complexes later then evaluated for their *in vitro* cytotoxic activity against several cancer cell lines such as the human lung carcinoma cell line (A549), human prostate cancer cell line (PC-3), and human breast cancer cell line (MCF-7). The compounds were screened using 3-(4,5-dimethylthiazol-2-yl)-2,5-diphenyltetrazolium bromide (MTT) cytotoxicity assay. Most of the diorganotin(IV) complexes showed great cytotoxic activity compared to the dithiocarbamate ligand itself for MCF-7 cell line. The dimethyltin(IV)chloride *N,N*-diethyldithiocarbamate (C7) was subsequently encapsulated in vesicles and its drug release profile was studied in phosphate buffered saline (PBS) at pH 7.4. The C7 was selected because it has the lowest IC_{50} value against MCF-7 cell line as well as lower than the IC_{50} value for cisplatin. The drug formulation (vesicles) was prepared by thin film hydration method. The formulated vesicles loaded with C7 were further characterized for

its percentage encapsulation efficiency, particle size, morphology, and release rate. The encapsulation efficiency was found to be high at more than 90%. Dynamic Light Scattering (DLS) was used to measure the particle size distribution. The results showed a size distribution of 119 nm with 100% intensity of vesicles loaded with C7. Field Emission Scanning Electron Microscopy (FESEM) was utilized for morphological analysis. The image showed an oblate shape vesicle with encapsulated C7. The complex was released from the vesicles up to 58% of the total loaded drug in two months. Based on the biological tests results and formulation outcomes, it can be concluded that diorganotin(IV) dithiocarbamate has a great potential in the pharmaceutical field for breast cancer therapies.

Keywords: diorganotin(IV) dithiocarbamate, *in vitro* cytotoxicity, encapsulation, vesicles, breast cancer.

SINTESIS, PENCIRIAN DAN KAJIAN ENKAPSULASI SEBATIAN KOMPLEKS DIORGANOTIN DITIOKARBAMAT

ABSTRAK

Sebatian organotin dan ditiokarbamat dikenali sebagai agen antikanser dan menunjukkan aktiviti sitotoksik seperti antiproliferatif dan antitumor. Penyelidikan ini tertumpu kepada sintesis, pencirian, dan kajian perumusan kompleks diorganotin(IV) ditiokarbamat untuk mengenalpasti potensinya pada sifat antikanser. Sepuluh sebatian kompleks diorganotin ditiokarbamat telah berjaya disintesis melalui tindak balas ligan ditiokarbamat dan dimetiltin(IV) diklorida. Kompleks tersebut dicirikan dengan spektroskopi inframerah transformasi Fourier (FT-IR), Nuklear Magnetik Resonan (NMR), spektroskopi cahaya nampak ultra-lembayung (UV-Vis) dan analisis elemen Karbon, Hidrogen, Nitrogen, dan Sulfur (CHNS). Struktur molekul dimetiltin(IV) *bis*(morfolinoditiokarbamat) telah ditentukan dengan kristalografi sinar-X, yang menunjukkan geometri trapeizodal-pencong dwipiramid. Ligan ditiokarbamat dan kompleks organotinnya kemudian telah diuji bagi aktiviti sitotoksik *in vitro* ke atas beberapa garis sel kanser manusia iaitu sel peparu (A549), prostat (PC-3), dan payudara (MCF-7). Sebatian tersebut telah disaring menggunakan ujian asai sitotoksisiti 3(4,5-dimetiltiazol-2-yl)-2,5-difeniltetrazolium bromida (MTT). Kompleks diorganotin telah menunjukkan aktiviti sitotoksik yang lebih baik berbanding ligan ditiokarbamat untuk garis sel MCF-7. Dimetiltin(IV)klorida *N,N*-dietilditiokarbamat (C7) kemudiannya telah dienkapsulasi dalam vesikel dan profil pelepasan ubat dalam larutan salin penimbal fosfat (PBS) pada pH 7.4 dikaji. C7 telah dipilih kerana ia mencatatkan nilai IC_{50} terendah untuk garis sel MCF-7 dan juga lebih rendah daripada nilai IC_{50} cisplatin. Rumusan ubat (vesikel) telah disediakan melalui teknik penghidratan filem nipis. Rumusan vesikel terkandung-C7 telah dicirikan lanjut untuk peratus kecekapan enkapsulasi, saiz zarah, morfologi, dan kadar pelepasan. Peratus kecekapan enkapsulasi didapati melebihi 90%.

Penyerakan cahaya dinamik (DLS) digunakan untuk mengukur taburan saiz zarah. Keputusan menunjukkan 119 nm dengan keamatan 100% bagi vesikel yang mengandungi C7. Mikroskopi elektron pengimbasan pancaran medan (FESEM) telah digunakan untuk analisis morfologi. Imej menunjukkan bentuk bulat membujur vesikel dengan berkapsul C7. Kompleks telah dilepaskan dari vesikel sebanyak 58% dari jumlah muatan ubat dalam tempoh dua bulan. Berdasarkan hasil ujian biologi dan hasil formulasi, dapat disimpulkan bahawa diorganotin(IV) ditiokarbamat mempunyai potensi yang besar dalam bidang farmaseutikal untuk terapi kanser payudara.

Kata kunci: diorganotin(IV) ditiokarbamat, sitotoksik *in vitro*, enkapsulasi, vesikel, kanser payudara.

ACKNOWLEDGEMENTS

I would like to express my deepest appreciation to all those who provided me the possibility to complete this thesis research. A special gratitude I give to my project research supervisors, Dr. Rusnah Syahila for the aspect of formulation and Dr. Lee See Mun in the preparation of compounds, whose have invested their full effort in guiding me in achieving the goal and contributed in stimulating suggestions and encouragement, helped me to coordinate my project especially in writing this thesis report successfully.

Furthermore I would also like to acknowledge with much appreciation the crucial role of the staff of Chemistry Laboratory Department, who gave the permission to use all required equipment and the necessary materials to complete the task characterization method such as Infrared (IR) spectroscopy, Nuclear Magnetic Resonance (NMR) spectroscopy, and UV-Vis spectroscopy. A special thanks goes to my team mate, Adibah and Nadia who help me to assemble the parts and gave suggestion in this research. Last but not least, I would like to thank my family for their support and encouragement over the years. Their prayers and love gave me the strength to get through in this journey. Also, I have to appreciate the guidance given by other supervisor Associate Professor Dr. Lo Kong Mun which also helped a lot.

TABLE OF CONTENTS

LIST OF FIGURES

LIST OF SCHEMES

LIST OF TABLES

LIST OF SYMBOLS AND ABBREVIATIONS

A549	:	Human lung carcinoma cell line
AChE	:	Acetylcholinesterase
C1	:	Dimethyltin(IV) *bis*(*N,N*-dimethyldithiocarbamate)
C2	:	Dimethyltin(IV) *bis*(*N,N*-diethyldithiocarbamate)
C3	:	Dimethyltin(IV) *bis*(*N*-methyl-*N*-phenyldithiocarbamate)
C4	:	Dimethyltin(IV) *bis*(morpholinodithiocarbamate)
C5	:	Dimethyltin(IV) *bis*(*N,N*-phenylpiperazinedithiocarbamate)
C6	:	Dimethyltin(IV)chloride *N,N*-dimethyldithiocarbamate
C7	:	Dimethyltin(IV)chloride *N,N*-diethyldithiocarbamate
C8	:	Dimethyltin(IV)chloride *N*-methyl-*N*-phenyldithiocarbamate
C9	:	Dimethyltin(IV)chloride morpholinodithiocarbamate
C10	:	Dimethyltin(IV)chloride *N,N*-phenylpiperazinedithiocarbamate
$CDCl_3$	:	Deuterated chloroform
$CHCl_3$	:	Chloroform
CHNS	:	Carbon, hydrogen, nitrogen, sulphur
CNS	:	Central nervous system
CTAB	:	Cetyltrimethylammonium bromide
DC-Chol	:	3beta-[N-(N',N'-dimethylaminoethane) carbamoyl] cholesterol
DL%	:	Percentage of drug loading
DLS	:	Dynamic light scattering
DMPC	:	Dimyristoylphosphatidylcholine
DMPG	:	Dimyristoylphosphatidylglycerol
DMSO	:	Dimethylsulfoxide
DMSO-d_6	:	Deuterated dimethylsulfoxide

DNA	:	Deoxyribonucleic acid
DPPC	:	Dimyristoylphosphatidylcholine
DSPE	:	1,2-Distearoyl-sn-glycero-3-phosphoethanolamine
DSPG	:	1,2-Distearoyl-sn-glycero-3-phosphoglycerol
DTAB	:	Dodecyl trimethyl ammonium bromide
EE%	:	Percentage of encapsulation efficiency
EPR	:	Enhanced permeability and retention
EtOH	:	Ethanol
ETU	:	Ethylenthiourea
FESEM	:	Field emission scanning electron microscopy
FTIR	:	Fourier transform infrared spectroscopy
GC	:	Gas chromatography
HeLa	:	Human cervix carcinoma cell line
HEP 3B	:	Hepatoma cell line
HepG2	:	Hepatoblastoma cell line
HPLC	:	High-performance liquid chromatography
IMR 32	:	Neuroblastoma cell line
IR	:	Infrared spectroscopy
K-562	:	Lymphoblastoma cell line
K562	:	Human myelogenous leukemia cell
L1	:	Sodium *N,N*-dimethyldithiocarbamate
L2	:	Sodium *N,N*-diethyldithiocarbamate trihydrate
L3	:	Sodium *N*-methyl-*N*-phenyldithiocarbamate
L4	:	Sodium morpholinodithiocarbamate
L5	:	Sodium *N,N*-phenylpiperazinedithiocarbamate
L929	:	Mouse fibrolast cell line

LUV	:	Large unilamellar vesicles
MCF-7	:	Human breast cancer cell line
MLV	:	Multilamellar vesicles
MPS	:	Mononuclear phagocytes system
MTT	:	3-(4,5-Dimethylthiazol-2-yl)-2,5-diphenyltetrazolium bromide
MTX	:	Methotrexate
NMR	:	Nuclear magnetic resonance spectroscopy
OND	:	Oligonucleotides
PBS	:	Phosphate buffer saline
PC-3	:	Human prostate cancer cell line
PCV	:	Phosphanated calixarene nanovesicles
PDI	:	Polydispersity index
PEG2000	:	Polyethylene glycol 2000
PEG	:	Polyethylene glycol
PLA	:	Polylactide
PTX	:	Paclitaxel
PVC	:	Polyvinyl chloride
SEC	:	Size exclusion chromatography
SEM	:	Scanning electron microscopy
SUV	:	Small unilamellar vesicles
TEM	:	Transmission electron microscopy
TGA	:	Thermogravimetric analysis
TPGS	:	Tocopheryl polyethylene glycol succinate
UV-Vis	:	Ultraviolet-visible spectroscopy

LIST OF APPENDICES

CHAPTER 1: INTRODUCTION

1.1 General Introduction

The chemistry of dithiocarbamates has been extensively studied as they show good stability of coordination with metals in different form. Due to its strong metal binding capacity, they give pharmacological effect on biological systems such as antibacterial properties, fungicidal, antifouling, and growth depressant (Gielen & Tiekink, 2005; Hogarth, 2012). Consequently, metal dithiocarbamates have attracted substantial interest on it. It is well-known that coordination of tin (Sn) has various geometries and coordination numbers such as mono-, di-, and triorganotin (Shahzadi & Ali, 2008; Tiekink, 2008). The different types of substituents and ligands attached to the Sn atom play an important role on the overall biological activity of the complexes (Tian *et al.*, 2005; Nath, 2008).

Organotin complexes have attained considerable interest in terms of their potential in biological activities such as antitumour, antibacterial, and antifungal agents. Currently, the significant interest reaches in organotin(IV) derivatives with dithiocarbamate ligands (Khan *et al.*, 2008; Khan *et al.*, 2015). This is because these organotin(IV) dithiocarbamate have shown great cytotoxicity activities against different types of tumour cells such as prostate, colon, lung, and breast (Alama *et al.*, 2009; Khan *et al.*, 2010). Therefore, these organotin(IV) dithiocarbamates later could load into nanocarriers as a potential therapeutic agent for targeted drug delivery in fighting cancer cells. The application of this synthetic organotin(IV) dithiocarbamates in drug delivery has a great prospective as the organotin(IV) complexes can bind to glycoproteins and directly interact with deoxyribonucleic acid (DNA) and initiate the apoptotic mechanism to induce cell death (Alama *et al.*, 2009; Arjmand *et al.*, 2014).

1.2 Research Background

Cancer is a well-known chronic disease with high rate of fatality. In mid-1960s, the introduction of metal complex, cisplatin by Rosenberg and his co-workers marked a huge impact towards cancer treatment in medical history. Cisplatin was the first metal compound used in the treatment of cancer (Cepeda *et al.*, 2007). However, the disadvantages of cisplatin in cancer treatments include severe side effects to the patients such as nausea, vomiting, nephrotoxicity, neurotoxicity, and ototoxicity (Kamaludin *et al.*, 2013). According to the Jongh *et al*. (2003), 42% of cancer patients suffered from nephrotoxicity pain when high dosage of cisplatin is administered. Therefore, compounds such as diethyldithiocarbamate, thiosulfate, mesna, and amifostine (WR-2721) were prescribed before or after cisplatin treatment to reduce the toxicity of cisplatin. Moreover, cisplatin has poor solubility in aqueous solution that may result in access restriction of tumour cells towards cisplatin. Besides, it may inflict damage to healthy cells since high dosage is required to reach the specific target cells.

Scientists have found that organotin compounds can induce cancer cell death at very low dosage and have better or similar potential than the widely currently-used drug cisplatin (Yamaguchi *et al.*, 2007; Alama *et al.*, 2009). This was supported by the great cytotoxicity activity of diphenyltin(IV) dithiocarbamate derivatives where they have lower IC_{50} value than cisplatin against the malignant tumour cell lines HEP 3B (hepatoma) and IMR 32 (neuroblastoma) (Kadu *et al.*, 2015). It was found that among of all metal complexes, Sn derivatives showed great potential in anticancer activity (Khan *et al.*, 2015). This might be due to the existence of easily hydrolysed chelating ligands producing intermediates such as $R_nSn^{(4-n)+}$ (n = 2 or 3) moieties, which could bind with deoxyribonucleic acid (DNA) and proteins (Nath, 2008).

There has been a growing interest in dithiocarbamates ligand due to its coordination ability into various form of coordination number with various metals. It was found that the coordinated dithiocarbamate showed greater biological activities than the uncoordinated one. For example, Sn dithiocarbamates which are more cytotoxic than the ligand itself exhibit capabilities as anticancer agents, antimicrobial agents, and insecticides. It has also been widely used as precursors for Sn sulphide nanoparticles production and as catalyst in rubber industry (Tiekink, 2008).

1.3 Significance of Research

This research offers some important insights in biological applications of diorganotin(IV) dithiocarbamate and its potential in drug delivery. Their potential in medical field may be further developed in cancer treatment since the organotin(IV) derivatives exhibit cytotoxic activity. The current chemotherapy drugs; cisplatin and platinum-based compounds have a significant drawback with their limited selectivity and high toxicity. Therefore, in this research, our main focus is on the non-platinum compound; specifically the organotin(IV) complexes that can induce apoptosis activity with better toxicity activity than cisplatin and give good interaction with DNA (Buac *et al.*, 2012). Numerous studies have attempted to explain the biological potential of organotin(IV) derivatives however, there have been no studies done yet on their encapsulation (Kadu *et al.*, 2015). Their performance in encapsulation studies such as release rate, encapsulation efficiency, and stability could be examined. Hence, a new line of low toxicity drugs with great anticancer properties could be obtained from this research.

The main problem found in current anticancer or chemotherapy drug is that they are targeting non-specific sites affecting all cells during division stage (Remesh, 2012). In order to achieve better efficacy of pharmaceutically active compounds (drug), the drug

can be encapsulated into drug carrier. The main role of drug carrier is to protect the drug from being damaged or released before reaching the target sites so that the therapeutic side effects can be minimized and the drug can reach the target cell effectively (Puri *et al.*, 2009). Moreover, with drug carrier, the constant release rate of drug can be controlled over a predetermined time. Thus, less frequent drug administration to the cancer patients and regulation of the drug concentration inside the body can be achieved. All these findings may give significant contributions to the pharmaceutical field.

1.4 Research Objectives

The objectives of this research were to prepare a series of mixed dithiocarbamate ligands and diorganotin(IV) complexes as well as to analyze and determine the structural features of the prepared ligands and the complexes. There are few techniques used to study the chemical structures and physical properties which include melting point measurement, the spectroscopic methods such as fourier transform infrared (FTIR) spectroscopy, nuclear magnetic resonance (NMR) spectroscopy, and ultraviolet-visible (UV-Vis) spectroscopy. X-ray crystallography and carbon, hydrogen, nitrogen, sulphur (CHNS) analysis also have been applied in present study for identification and confirmation on the chemical structures of the synthesized ligands and complexes.

The ligands and the diorganotin(IV) complexes were then screened for their anticancer activity and the cell lines used in this study include human lung cancer cell line (A549), human prostate cancer cell line (PC-3), and human breast cancer cell line (MCF-7). Furthermore, spectroscopic characterizations, *in vitro* anticancer activities, and encapsulation of the diorganotin(IV) dithiocarbamate were also investigated for drug release studies. The best candidate was selected based on the highest cytotoxic activity against all cancer cell lines.

1.5 Thesis Outlines

The overall structure of this thesis consists of five chapters; including the introduction chapter. Chapter 1 presents an introduction to research background, significance, and the objectives of the research. The motivation and the problem statement were included in the research significance. Chapter 2 begins by laying out the literature background of dithiocarbamate ligands and its organotin complexes with its potential properties. A brief introduction on encapsulation studies such as drug carriers, administration of drugs, and its applications were also explained. Chapter 3 describes the materials preparations and experimental procedures run throughout this work. The synthesis route features in the experiments and the characterization methods were also explained. Chapter 4 discusses the overall findings from the characterization techniques used throughout this work. The final chapter concludes the research output and the proposal of future actions in regards to the objectives of this thesis. The Appendix shows supplementary data correlated to the experimental work and results.

CHAPTER 2: LITERATURE REVIEW

2.1 General Introduction

Widely-known as a vital class of metal coordinating agents, the dithiocarbamate ligand is an effective ligand for metals. The organotin compounds with oxygen (O), nitrogen (N), and sulphur (S) donor ligands have been previously studied (Khan *et al.*, 2008; Shang *et al.*, 2008) due to their configuration structures and the resulting biological activity. Among the ligands, dithiocarbamates are of a particular interest as the coordination of Sn moieties with sulphur ligands is more stable than the coordination with the nitrogen and oxygen ligands (Fuentes-Martínez *et al.*, 2009; Safari *et al.*, 2013). The application, as well as the biological potential of the dithiocarbamate ligands and the organotin dithiocarbamates were reviewed in this chapter. In addition, its application in pharmaceutical and its performance in encapsulation studies were also addressed.

2.2 Dithiocarbamate Chemistry

The basic formula of dithiocarbamate anions is $^{-}S_2CNR'_2$ which consists of half-amides of dithiocarbonic acid (Singh & Kaushik, 2008). They can be synthesized by the reaction of carbon disulphide with amine in the presence of base to give ammonium or alkali metal salts. **Figure 2.1** shows the general structure and reaction scheme of the dithiocarbamate production (Tiekink, 2008).

Dithiocarbamates are versatile ligands and possess the ability to form complexes with most elements. The presence of two sulphur atoms donor lead to strong metal binding properties. They can stabilize a variety of oxidation states and coordination geometries such as monodentate, bidentate or multidentate to two or even three metal centres (Heard,

2005). Since they have a strong metal binding capacity, dithiocarbamate ligands can also act as enzymes inhibitors and may also influence the biological systems.

$$R_2NH + CS_2 + NaOH \longrightarrow R_2NCS_2^-Na^+ + H_2O$$

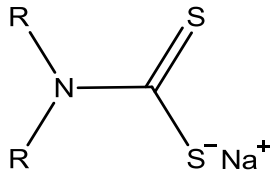

Figure 2.1: Reaction scheme and general structure of dithiocarbamate.

Dithiocarbamate ligands are considered as soft donors as they show excellent coordination ability and have the tendency to share electrons between nitrogen, sulphur, and metal ions (Khan *et al.*, 2015; Abu-El-Halawa & Zabin, 2017). This property is due to the backbone structure of the ligands which is a result of simple substituent exchange at the nitrogen atom that enables it to form stable complexes with various metal compounds.

2.2.1 Dithiocarbamate Ligands

In therapeutic applications, dithiocarbamate ligands have been of particular interest to researchers due to their antibacterial, antiviral, and antitumour properties. The general structure of dithiocarbamate including its cyclic derivatives form such as piperidine, morpholine, and piperazine have shown antimicrobial activity. For example, *N*-alkylthiazolidine-2-thiones possess antifungal activity and chalconedithiocarbamates exhibit antiproliferative activity (Hussein *et al.*, 2001; Sağlık *et al.*, 2014). It was found that dithiocarbamate compounds such as ethylenthiourea (ETU) and propylenthiourea (PTU) are the key group of fungicides, where it gave effect on approximately 400 pathogens of more than 70 crops. They are also found as effective catalysts for photopolymerization and rubber vulcanization (Blasco *et al.*, 2004; Hassan & Zayed, 2014). Recently, dithiocarbamate compounds play a key role in the pharmaceutical field

due to their unique molecular structure with the lipophilic property. This property is important for the delivery of central nervous system (CNS) drugs to their target action sites through the blood-brain barrier. Hence, dithiocarbamates can be considered as acetylcholinesterase (AChE), a potential inhibitors for the treatment of Alzheimer's disease (Tokuyama *et al.*, 2001; Sağlık *et al.*, 2014).

Dithiocarbamates have the ability to regulate key proteins such as in the process of apoptosis, transcription and degradation which is not only significant as a potential anticancer agent but also useful in the treatment of cocaine addiction, viral diseases, and inflammation. In correlation to anticancer potential, dithiocarbamate derivatives; *N,N*-dimethyldithiocarbamate and ethylsarcosinedithiocarbamate, have also been used as proteasome inhibitors where they are responsible in blocking the action of proteasome in cancer therapy (Buac *et al.*, 2012). Besides, it was also reported in literature that diethyldithiocarbamate anion, Et_2CNS_2, may be applied to remove excess copper known as Wilson's disease. Also, it alleviated poisonous effect of some substances on the kidneys associated with platinum-based chemotherapy (Ferreira *et al.*, 2012). Apart from their use in medical applications, dithiocarbamate can also be used as linkers to improve electron transport properties in molecular wire junctions. In addition, they can also be utilized to inhibit corrosion and used as an additive to enhance the quality of lubricants (Abu-El-Halawa & Zabin, 2017).

Other than that, dithiocarbamates can be used as chelators to remove metals such as lead (Pb), copper (Cu), and zinc (Zn) from polluted water since it has good binding abilities that can precipitate out metal ions as complexes. This is due to dithiocarbamate's tendency to share electrons with nitrogen, sulphur, and metal ions. Thus, it helps to reduce serious environmental problems that can cause adverse health effects. It has been shown that diphenyldithiocarbamate ligand is more efficient in removing metals rather than

diethyldithiocarbamate. This is due to its more stable bonding capacity with heavy metal ions (Abu-El-Halawa & Zabin, 2017). The coordination of dithiocarbamate ligands with organotin compounds have attract considerable interest recently due to their good coordination stability as both compounds displayed great potential in biological activity, chemical process, and pharmaceutical field.

2.3 General Overview of Organotin

Organotins are compounds with at least one organic substituent linked directly to Sn atom via the carbon atom of the organic substituent. There are two types of organotin compounds; the organotin(II) and the organotin(IV). Since it has two stable oxidation states +II and +IV, the organotin(II) is less stable and tends to polymerise and easily oxidised to organotin(IV). Organotin(IV) compounds possess sp^3 hybridization for its valence orbital, hence forming the tetrahedral oriented bonds. There are four types of organotin(IV) compounds; the mono-, di-, tri-, and tetraorganotins as shown in **Figure 2.2**, which are represented by the formula R_nSnX_{4-n} (n=1–4). These coordination structures depend on the utilisation of multifunctional dithiocarbamate ligands which include the role of alkyl (R) groups in dithiocarbamate ligands. For instance, this R groups can take part in hydrogen bonding or act as donor to develop new coordination to tin (Tiekink, 2008; Castrejón-Antúnez *et al.*, 2016).

Organotin(IV) compounds are among the most widely used organometallic material and have been applied into various fields such as industrial and agricultural. Their applications include as pesticides, fungicides, and antifouling agents. Dimethyltin(IV) dichloride was also used as a precursor to form thin surface films of SnO_2 on glass. On the other hand, some dialkyltin compounds play a role in cancer chemotherapy and they possess lower toxicity when compared to triorganotin and tetraorganotin. Therefore,

dialkyltin needs substituents such as dithiocarbamate and halides to exhibit better anticancer activity rather than by itself (Awang *et al.*, 2011).

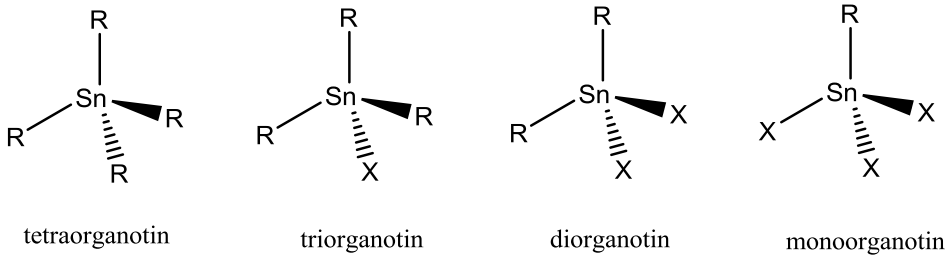

Figure 2.2: Structure of organotin.

Diorganotins have low antifungal activity, low antibacterial activity, and also less toxic than triorganotin and tetraorganotin. Diorganotins are commonly used in polymer manufacturing; as PVC heat stabilizers and as a catalyst in the production of polyurethane. Monoorganotins on the other hand show no biological activity and have very low toxicity to mammals. Methyltin, butyltin, and octyltin have also been used as PVC heat stabilizers (Singh & Bhattacharya, 2012).

2.3.1 Organotin(IV) Dithiocarbamate

The most interesting organotin complexes are tetra*kis*(dithiocarbamate)tin(IV) complexes because they can develop different bonding styles with the dithiocarbamate ligands, such as monodentate, chelating bidentate or multidentate with two or three metal centres as shown in **Figure 2.3** (Coucouvanis, 1979). The figure shows the coordination for (a) single metal with a bidentate; (b) two metals with a monodentate and a bidentate; (c) three metals but all are in monodentate coordination; (d) single metal with a monodentate; and (e) two metals and both are monodentate. Another interesting complex is diorganotin(IV) dithiocarbamate, $R_2Sn(S_2CNRR')_2$ as per this thesis focus. These species have highly distorted trigonal bipyramid molecular structure of Sn complex geometry. It has active lone pair of electrons at the equatorial position to the other three substituents bonds and the two long tin to sulphur (Sn-S) bonds are displaced away from

the lone pair in pseudo-axial positions to form a stable coordination compound (Tiekink, 2008).

Figure 2.3: Coordination of ligands.

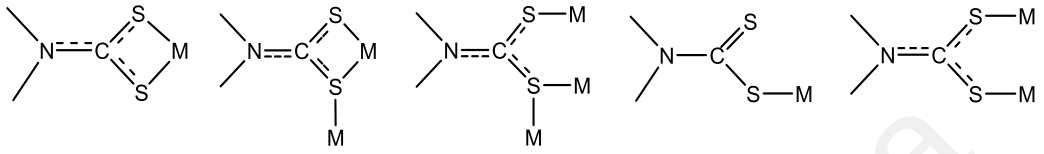

(a) (b) (c) (d) (e)

Organotin(IV) compounds could be developed as cancer chemotherapy since they have apoptosis properties. Apoptosis process is responsible in attaining and sustaining the health of the body by removal of old cells, redundant cells, and unhealthy cells. These compounds potentials in pharmaceutical include antiproliferative, antitumour, and anticancer drugs (Qureshi *et al.*, 2014).

The biological activities of organotin(IV) complexes typically depends on the number and the environment of ligands attached to the central Sn atom. For example, lower homologues such as ethyl and methyl attached to organotin(IV) complexes will produce the most toxic drug. The toxicity will gradually reduce as the substituents increase from propyl to octyl (Sirajuddin *et al.*, 2014). However, the resulting toxicity will differ with the presence of aromatic ring in the complex as the presence of phenyl group will increase the toxicity. Complexes with triphenyl-, dibutyl- and trimethyl- attached to organotin(IV) had been previously studied and the order of the compounds in term of its antifungal and antibacterial activities is triphenyltin > dibutyltin > trimethyltin (Awang *et al.*, 2010).

A few dithiocarbamate complexes namely dimethyltin(IV), dibutyltin(IV), and triphenyltin(IV) methylcyclohexyldithiocarbamate were studied for antibacterial properties in different concentrations against pathogenic bacteria. Awang *et al*. (2011) reported that complexes with phenyl groups showed more inhibitory effect on Gram-

positive bacteria which are *Staphylococcus aureus* and *Salmonella typhimurium*. It can be concluded that the antibacterial activity of triphenyltin(IV) dithiocarbamate is much higher against the tested bacteria as compared to dimethyltin(IV) cyclohexyldithiocarbamate. The phenyl group results in the electron delocalization that increase the chelating ability of the ring system consequently increasing the lipophilicity level of the compound. Thus, the compound can be easily absorbed by the bacterial membrane (Awang *et al.*, 2011).

For antifungal activity, triorganotin(IV) dithiocarbamates have shown great activity against the tested fungi as compared to diorganotin(IV) dithiocarbamates. In the following examples, the organotin(IV) complexes were found to show greater activity than the ligand itself. For instance, organotin(IV) complex of 2-phenylethyl dithiocarbamate are more active than the ligand itself against the tested fungi; *Rhizoctonia solanii* and *Sclerotium rolfsii* as the phenylethyl attached to the Sn increases the antifungal activity (Singh & Kaushik, 2008).

In addition to that, studies have shown that fluorine can be a useful substituent in organotin(IV) dithiocarbamates. Due to its small steric size, fluorine has been used as hydrogen replacement in many biologically active molecules. The introduction of fluorine into organotin(IV) dithiocarbamate has shown an increase in metabolic, oxidative, and thermal stability. Fluorine usually increases lipophilicity of the compound as the bond between carbon and fluorine is much stronger than carbon-hydrogen bond. Therefore, the replacement with fluorine improves the biological and chemical stability of the compounds (Noureen *et al.*, 2015).

Cytotoxicity test of the dibutyltin(IV) dithiocarbamates showed moderate antitumour activities whereas, dimethyltin(IV) dithiocarbamates showed very poor or no activity at certain concentrations. Since dibutyltin(IV) dithiocarbamates had shown antitumour

potential in human Jurkat, hepatoblastoma cell line (HepG2), lymphoblastoma cell line (K-562), and mouse fibroblast cell line (L929), it may be possible to be developed as antitumour agents after further research and clinical trials (Khan *et al.*, 2015). It was found that the complexes of dithiocarbamates also exhibit higher activity against cancerous cells in comparison to the corresponding compounds of other sulphur containing ligands such as thiones (Urgut *et al.*, 2016).

The cytotoxic activities were also exhibited in the organotin(IV) complexes from the reaction of *N*-benzylisopropyldithiocarbamate with dimethyltin(IV) chloride, dibutyltin(IV) chloride, and triphenyltin(IV) chloride that form bidentate chelation with the organotin(IV) moieties. The screening results of cytotoxic activity reveal that triphenyltin(IV) complex has the highest activity against the HepG2 cell line where the IC_{50} value is the lowest among all the compounds. The cytotoxicity activities of the complexes can be arranged as follows: triorganotin(IV) > diorganotin(IV) > monoorganotin(IV), being triorganotin(IV) is the most cytotoxic. Triphenyltin(IV) complex has shown more significant cytotoxic activity but slightly lower to the reference drug which is etoposide. It was believed that it has substantially high potential in the medicinal area with further research (Awang *et al.*, 2010).

Additionally, Safari *et al*. (2013) reported that compound with phenyl group exhibited the highest cytotoxic activity. Triphenyltin(IV) (morpholine-1-carbodithioate) and tribenzyltin(IV) (morpholine-1-carbodithioate) were evaluated against human cervix carcinoma cells (HeLa) and human myelogenous leukemia cells (K562). Both compounds showed higher cytotoxic activity than cisplatin. Triphenyltin(IV) (morpholine-1- carbodithioate) is the most active complex against the assessed tumour cell lines. The results indicate that it is 171 times more active in K562 cells than cisplatin.

It can be concluded that even with one small structural change; for example the exchange of phenyl with benzyl group can greatly affect the cytotoxic (Safari *et al.*, 2013).

Finally, Fuentes-Martinez *et al*. (2009) reported that chlorodiphenyltin(IV) dithiocarbamate complexes were used as a chromogenic sensor of anion binding since free dithiocarbamate anion has intrinsic chromogenic properties. Apart from that, chromogenic sensors can be obtained by linking the dithiocarbamate groups with fluorescent moieties such as anthracene. As a result, the organotin(IV) complexes with these substituents can detect the presence of oxygen donor anions at very low concentrations by shifting the metal-coordinated ligands (Fuentes-Martínez *et al.*, 2009).

2.3.2 Characterization of Diorganotin(IV) Complexes

The dithiocarbamate ligands and its diorganotin complexes can be characterized using various tools such as melting point measurement, fourier transform infrared (FTIR) spectroscopy, nuclear magnetic resonance (NMR) spectroscopy, ultraviolet-visible (UV-Vis) spectroscopy, carbon, hydrogen, nitrogen, and sulphur (CHNS) elemental analysis, thermogravimetric analysis (TGA), and X-ray crystallography. Melting point measurement was conducted as it is one of the fastest ways to test if the desired product was obtained. Besides, the melting point range provides indicator on the purity of sample. The spectroscopic methods such as FTIR, NMR, and UV-Vis spectroscopy were applied for identification and confirmation on the chemical structure of the compounds. Electronic properties of the compounds were studied using UV-Vis spectroscopy. CHNS elemental analyzer was utilized for determination of percentage of composition of elements C, H, N, and S in complexes. Single X-ray crystallography is very useful for determination of structural and molecular packing of crystalline compounds. TGA also can be performed to analyze the change of mass in compounds.

2.3.2.1 Fourier Transform Infrared (FTIR) Spectroscopy

FTIR spectroscopy is an instrumental method used to determine and identify the presence of structural units, including functional groups and its vibration characteristics. In general, the functional groups that can be found in organotin(IV) complexes are Sn-O, Sn-C, C-Br, -CN, and C-S. Most of the stretching vibrations correspond to the Sn atom were found in the frequencies' range from 200 cm^{-1} to 900 cm^{-1}. Typically, the frequencies of ν_{as}(Sn-C) and ν_{s}(Sn-C) were found in the range of 500–600 cm^{-1} and 470–530 cm^{-1} respectively. The modifications in the coordination number of the Sn atom do not affect the Sn-C stretching vibrations. On the other hand, the Sn-X (X=Cl, Br, F) stretching modes will be affected by the alteration in coordination number of Sn from 4 to 6. Apart from that, the Sn-O stretching modes for diorganotin complexes are mostly found at 600–700 cm^{-1} frequencies. The band showed strong absorption, while the weaker or medium band intensity around 400–500 cm^{-1} frequencies can be pointed as Sn-N stretching modes (Sainorudin *et al.*, 2015).

The three most important absorption regions for organotin(IV) dithiocarbamate complex are:

i) absorption at 1450–1550 cm^{-1} corresponding to C=N functional group.

ii) absorption at 950–1050 cm^{-1} corresponding to C-S functional group.

iii) absorption at 350–450 cm^{-1} that correspond to vibration of Sn-S functional group.

2.3.2.2 Nuclear Magnetic Resonance (NMR) Spectroscopy

NMR gives information about the number of magnetically distinct atoms of the type of each hydrogen nuclei (protons) being studied. The distinct types of each protons can be determined depending on the nature of the proton environment whether it is a singlet,

duplet, triplet, and multiplet. Additionally, the number of non-equivalent carbon and the nature of the carbon atoms; whether it is a methyl, methylene, aromatic, carbonyl, and so on can be determined by using carbon NMR. In summary, carbon NMR can provide direct information on the carbon skeleton of a particular molecule. Frequently, NMR and FTIR data are combined together for complete determination on the structure of an unknown molecule.

Organotin complexes can be characterized by using the ^{1}H-, ^{13}C- and ^{119}Sn-NMR spectroscopies in order to analyze their fluxional behaviour. There are many factors that affect the chemical shift, δ in ^{119}Sn NMR such as the oxidation number of Sn, the substituents attached to the Sn atom, the coordination number of the Sn atom and the geometric configuration at the Sn centre (Jastrzebski *et al.*, 1991). The chemical shifts of ^{119}Sn-NMR indicate the different coordination number of the central Sn atom, for example; four-coordinate compound have a range of +200 ppm to −60 ppm, five-coordinate compound is assigned when the range is between −90 ppm to −190 ppm, and six-coordinate compound have a range in between −210 ppm to −400 ppm (Holeček *et al.*, 1986). Structural information of the complexes can be obtained from two parameters; chemical shifts, δ (usually expressed in ppm) and coupling constant, J (usually expressed in Hz).

2.3.2.3 Ultraviolet-visible (UV-Vis) Spectroscopy

UV-Vis spectroscopy can be employed to observe the electronic transition present in a compound. Some molecules and functional groups are transparent in the UV-Vis portion of the electromagnetic spectrum; the wavelengths region of UV-Vis is 190 nm to 800 nm. Typically, organotin(IV) dithiocarbamate complex will generate two important bands; the first one from the C=N bond and the other one from sulphur atom which contains lone

pairs of electron. These bands appearance confirm the formation of the complex. Another band may appear in the spectrum due to metal-ligand charge transfer. On the other hand, dithiocarbamates normally show three bands in UV region which came from the π-π* transition for N-C=S, π-π* transition for S-C=S and n-π* transition corresponding to the lone pair of electron in sulphur atom (Ekennia *et al.*, 2015; Sainorudin *et al.*, 2015).

2.3.2.4 X-ray Crystallography

In X-ray crystallography, diffraction method particularly utilized for structural determination of various molecules and self-assemblies. This technique is used to determine the positions of the atoms and ions that make up a solid compound by providing a description of structures in terms of features such as bond lengths, bond angles, and the relative positions of ions and molecules in a unit cell. This structural information is interpreted in terms of atomic and ionic radii that lead to structural prediction. Diffraction can be defined as the interference of waves as a result of obstruction (an object) in their path (Tiekink, 2008).

2.3.2.5 Thermogravimetric Analysis (TGA)

TGA is one of the thermal analysis methods that can be used to analyze the change in a property of a sample (e.g. the sample's mass) that induced by heating. The sample is usually a solid and the changes that occur include melting, phase transition, sublimation, and decomposition. The measurements are carried out using thermobalance; which consists of an electronic microbalance, a temperature programmable furnace, and a controller, that enables the sample to be simultaneously heated and weighed. TGA is very useful for the study of desorption, decomposition, dehydration, and oxidation process.

2.3.2.6 Carbon, Hydrogen, Nitrogen, and Sulphur (CHNS) Elemental Analyzer

The purpose of CHNS elemental analyzer is to determine the percentage of composition of carbon, hydrogen, nitrogen, and sulphur. The analyzer can handle various

types of sample in various state including solid, liquids, volatile sample, and viscous sample. The method involves is the combustion process; where carbon will be converted to carbon dioxide, hydrogen to water, nitrogen to nitrogen gas or oxides of nitrogen, and sulphur to sulphur dioxide. There are a variety of techniques to detect these gases. One of them is via gas chromatography (GC) separation followed by thermal conductivity. Another technique is by using a partial GC separation (frontal chromatography) which then followed by thermal conductivity detection (only CHN but not S). Lastly, a series of separate infrared and thermal conductivity cell can also be carried out to detect each of the elements in the compound.

2.4 Encapsulation Studies

Encapsulation is defined as a technique for packaging the bioactive molecules into inert and non-toxic carriers that have the capability of releasing the active ingredients at a controlled rate under certain conditions (Puri *et al.*, 2009). Generally, the development and application of drug carrier are focused on the encapsulation studies. It is important to enhance the absorption, constancy, and concentration of drug in target tissues. With that, the drug release at the target site can be controlled and improved for long-term period release (Kayser *et al.*, 2005; Kubik *et al.*, 2005). In order to acquire a more selective approach to drug delivery, the protection of drug should be escorted with non-targeted tissue. The drug can then reach the target cell while reducing the damage inflicted to the healthy cells (Papadimitriou & Bikiaris, 2009; Tarvirdipour *et al.*, 2016).

Since various literature works had reported that diorganotin(IV) dithiocarbamate compounds possess great anticancer properties, further analysis of the compound in encapsulation studies have become of great interest in order to establish their potential as an anticancer drug even though the mechanism of its biological action have not yet prevalent. Cancer is one of the most chronic disease in the world. It is well-known that

chemotherapy is one of the universal cancer treatments. Chemotherapy is an introduction of cytotoxins into the bloodstream. Most of current drugs (e.g. paclitaxel) are poorly soluble in the bloodstream (Sun *et al.*, 2012). This means that high dosage of drugs is needed to combat the tumour cells.

New drug invention is required to overcome or reduce the toxicity of current drugs towards the body. There are five different formulation methods to obtain sustainable drugs delivery system as reviewed by Lavik *et al.* (2013). The first approach is by enclosing the drugs with molecules so that the drug's residence time at the target cell will be longer. For example, by attaching the polyethylene glycol (PEG) molecules, the circulation time of drug in the bloodstream can be enhanced since PEG will create a highly hydrated volume around the drug (Harris & Chess, 2003). The second method is the encapsulation of drug in reservoir system incorporates with membrane where the drug is allowed to diffuse across the device and to the surrounding tissues. Using this method, many drugs can be delivered over a long period of time (Langer, 1983). The third approach is matrix-based system where the drug is mixed with polymers that initiate the entrapment of drug in polymer matrix. A longer release of drug can be achieved if they have stronger interaction between each other (drug and polymer). Other than that, the osmotic system has been established where water will diffuse into the matrix as a consequence of swelling and initiate drugs release through diffusion. The last approach is the pump system. This method allows periodic release of drugs for large scale medication.

In encapsulation studies, knowledge on path administration of drug is essential to design an efficient drug delivery system. There are various routes of drug administration, for example; via oral or transdermal administration. Different types of drug carrier such as hydrogels, nanotubes, vesicles, and liposomes are suitable for different routes of

administration. Their physical characteristics such as size and shape can provide the insight in deciding the suitable route for administration of drug.

2.4.1 Administration of Drugs

There are three major routes for anticancer drug administrations; intravenous, oral, and transdermal administration. The different routes of drug administration play a specific role in maintaining the bioavailability of the drug in the body. They have their own pros and cons effects towards our body. One of the most versatile methods in drug administration is intravenous administration where the drug is infused directly into a vein through needle or tube. As a result, it provides quick access of the drug to the bloodstream with high adsorption rate. The after-effect may be painful; however, it can provide immediate action in the body. Drugs can be administered to unconscious patients through this method. The common drug carriers for this administration route are nanotubes, polymeric micelles, vesicles, and emulsion (Dufes *et al.*, 2004; Immordino *et al.*, 2006; Hussen & Heidelberg, 2016).

Drugs can also be consumed orally. In this route, absorption may occur along the gastrointestinal tract where degradation of drug by gastric acid may occur. Besides, the drug will not completely be absorbed and will take a longer time for it to reach the target sites in the body (Verma *et al.*, 2010). Unlike intravenous administration, high dosage of drugs can be administered and it can easily be absorbed into the bloodstream. It is a more flexible method where continuous infusions can be provided over a few days or for weeks at a time.

In transdermal administration, the active ingredients are applied on the surface of the skin for its systemic effect. Normally, high dosage of drug (more than 10 mg) is difficult to absorb through the skin due to the poor permeability of skin. Additionally, not all types of compounds can permeate through skin layer. The low permeability of skin limits the

application of drug carrier to only nanoemulsions, emulsions, and gels (Jhawat *et al.*, 2013). Hence, in this research, the suitable administration route for the prepared vesicles (at the ideal size of below 200 nm) is via intravenous injection (Singh & Lillard, 2009).

2.4.2 Drug Carriers

Drug carrier is a substrate used to transport active ingredients and simultaneously helps to improve the selectivity and shelter the active ingredient *en route* to its target cells. There are various ways to improve the performance of a particular drug, for instance, by altering the path of drug administration, or by chemical structural modification of the drug itself or by adjusting the amount of dosage. By tuning the carrier, it is possible to invent a drug that have long-lived circulation and more biocompatible with the target cells, and it also enable high drug loading. Drug carrier was invented nearly three decades ago in 1982 to accomplish various goals such as stability, bioavailability, and inhibition of drug interactions. With this invention, drug molecules with large molecular weight such as proteins and peptides can be delivered to the target sites with the help of drug carrier system. Drugs carriers assist in accurately targeting a specific site of a particular cells or organs without interrupting other organs (Srikanth *et al.*, 2012). In addition, it helps to slow down the release rate of the drug and reduce the risk of drugs' decimation along the path of its target site (Puri *et al.*, 2009). There are various types of drug carriers such as vesicles, liposomes, microspheres, nanoparticles, and nanotubes.

One of the most widely used drug carriers in drug release formulations is vesicles. This is because it has greater stability where it can encapsulate both hydrophilic and hydrophobic drugs due to the presence of bilayer consists of hydrophilic and hydrophobic segments (Manosroi *et al.*, 2012). Since vesicles has the possibility to lower the release rate of drug and remain sustained in the body, appropriate amount of drug concentration can be controlled in a longer period of time. Also, it has high cell penetration efficiency,

thus, pharmacological activity and pharmacokinetics properties of drugs could be improved. Antibody or modified chemical structure of active ingredients may be attached to vesicles for the specificity of drug delivery (Laouini *et al.*, 2012; Zhang *et al.*, 2013; Tavano *et al.*, 2014).

In addition, the similarity of vesicle's membrane structure to cell membrane means that the vesicles have good biofilm compatibility and cell permeability (Li *et al.*, 2015). The common systems found in vesicles are cationic, anionic, and non-ionic where different types of vesicles have a significantly different target in drug delivery. Therefore, each of the vesicles have their own ability to localise the activity of drug at the site or organ of action (Jain *et al.*, 2014).

Cationic vesicles have been proven to be an anti-infective agent and also effective in transfection of DNA into the cell. An increase of drug concentration around the tumour area can be observed as a result of electrostatic interaction between the cationic vesicles and negatively charged molecule on the tumour cell such as proteoglycans, glycoproteins, and anionic phospholipids. Anionic drugs can also be carried by this positively charged cationic vesicle and the carrier can form complex with anionic genetic molecules for delivery to the cells, thus, enhancing the permeation of gene across the membrane (Bergstrom & Garamus, 2012; Muzzalupo *et al.*, 2017). However, the disadvantage of cationic vesicle is the structural instability where it could be degraded by hydrolysis, or oxidation that leads to drugs leachate and aggregation during storage. They possess high toxicity in high dosage and their transfection activity reduced with time (Talegaonkar *et al.*, 2006). One of the applications for cationic vesicles is in cosmetic formulations where it is applied through transdermal administration. Due to its amphiphilic properties, its capacity for skin penetration is high (Cevc, 2004) . Since skin surface can sustain the

negative charge, the positively charged vesicles may increase the infusion rate of cosmetics through the skin (Dragicevic-Curic *et al.*, 2010).

Another vesicles system is non-ionic where the vesicles structure consists of highly ordered bilayer made up of non-ionic surfactant surrounded with aqueous solution. They are comprised of polar and non-polar segments where the hydrophobic tails of surfactant facing away from the aqueous part while its hydrophilic head facing towards the aqueous space. Non-ionic vesicles is chemically stable as they require no special conditions (e.g. low temperature or inert atmosphere) for protection or storage, and low production cost (Talegaonkar *et al.*, 2006). Generally, they have low toxicity and less likely to cause haemolysis, also less irritation to cellular surface and can be maintained at near physiological pH in solutions. Furthermore, this non-ionic vesicle can enhance the solubility of some insoluble drugs such as methotrexate (MTX), particularly for oral and transdermal drugs as well as improving therapeutic performance of drugs by sustaining the release rate (Azmin *et al.*, 1985). They can act as wetting agents, solubilisers, emulsifiers, and permeability enhancers. They pose wide pharmaceutical applications in drug delivery system such as in pulmonary delivery, transdermal delivery, cancer chemotherapy, and vaccine/antigen delivery. Comparisons of the vesicle carriers bring about the conclusion that negatively charged vesicles have shorter circulation in bloodstream than neutral (non-ionic) vesicles while positively charged carriers are toxic and rapidly removed from the circulation (Funato *et al.*, 1992).

Other than that, mixed vesicles system has also been applied in drug formulation studies. According to Lainez *et al*. (2004), mixed vesicles showed better application performance than the one surfactant vesicle system (Lainez *et al.*, 2004). For example, cetyltrimethylammonium bromide (CTAB)-dimethyl alkyl phosphine oxide mixed system exhibited lower critical micellar concentration than both its cationic and non-ionic

components. This indicates that less surfactant is needed to saturate the interaction interface of the surfactant molecule and the tumour cell surfaces (Negm & Sabagh, 2011). There are many types of mixed surfactant vesicles comprising of anionic/cationic, non-ionic/cationic, zwitterionic/cationic, cationic/cationic, and polymer/cationic (Geng *et al.*, 2017). In this research, the incorporation of cationic surfactant to non-ionic surfactant will actually assist the formation of vesicles and stabilize its bilayer structure. For example, it was reported that polyethylene glycol (PEG) together with 3beta-[N-(N',N'-dimethylaminoethane) carbamoyl] cholesterol (DC-Chol), 1,2-distearoyl-sn-glycero-3-phosphoethanolamine-N-methoxy-polyethylene glycol 2000 (DSPE-PEG2000) and non-ionic surfactant-Span have been used to improve the stability and cellular delivery of oligonucleotides (OND) (Huang *et al.*, 2008). Due to the enhancement in the carrier stability, mixed vesicles system of cationic/non-ionic have been used for drug formulation in this work.

There are three common sizes of vesicles which are small unilamellar vesicles (SUV); ≤0.1 μm, large unilamellar vesicles (LUV); 0.1-10 μm, and multilamellar vesicles (MLV); 0.1-0.3 μm (Perrie *et al.*, 2013). Numerous methods had been introduced to prepare the vesicles such as thin film hydration, ethanol injection, homogenisation, and microfluidics. Different preparation methods will produce different types of vesicles. For example, ethanol injection method will produce small unilamellar vesicles (SUV). Normally, thin film hydration method will produce either multilamellar vesicles (MLV) or large unilamellar vesicles (LUV) (Popovska *et al.*, 2013). Additional techniques such as sonication and extrusion can be introduced to produce small unilamellar vesicles (SUV).

2.4.3 Preparation Method of Drug Carrier

The main consideration to take into account in selecting a suitable method for drug formulation is achieve an efficient drug encapsulation and reducing particle size

distribution in order to obtain a stable carrier (Popovska *et al.*, 2013). The most common method used for drug carrier preparation is thin film hydration method. This method offers a quick and straightforward procedure in drug formulation preparation. Generally, a dry thin film of drug and surfactant mixtures was deposited on the wall of a flask. Then, the thin film was hydrated by adding buffer solution under agitation to form drug suspension (Olson *et al.*, 1979; Hussen & Heidelberg, 2016).

Another method that can be used to prepare drug carrier is ethanol injection. In this method, the vesicles will be briefly dissolved in ethanol before rapidly injected into buffer solution and vesicles with small particle size can be obtained. It was a simple, rapid, and non-invasive method. However, this technique will produce dilute vesicle suspension that will lead to low encapsulation efficiency (Szoka & Papahadjopoulos, 1980). Next is the reverse-phase evaporation technique. The film will be formed by removing the organic solvent under reduced pressure. This system eliminated with nitrogen and the vesicles are re-dissolved in a second organic phase. Then the organic solvent is eliminated and the system is maintained under continuous nitrogen blanket. Indisputably, high encapsulation efficiency will be obtained using this technique. However, it may affect environment and human health as this method make used of large amounts of organic solvent which is harmful and toxic (Laouini *et al.*, 2012). There are numerous other methods that have been used to prepare vesicles; such as the detergent dialysis, calcium induced fusion, nanoprecipitation, and emulsion techniques.

Based on the techniques stated above, thin film hydration was chosen to prepare the vesicles due to the method's simplicity and the applicability of it in this encapsulation studies. In general, thin film hydration is a simple and well-established method that enables the encapsulation of a variety of compounds (Szoka & Papahadjopoulos, 1980).

2.4.4 Characterization of Vesicles

The physical characteristics of vesicles are specifically controlled by its preparation method, i.e. thin film hydration, ethanol injection, and nanoprecipitation method. Usually, the most significant parameters in drug carriers are size distribution, surface charge, polydispersity index (PDI), percentage of drug encapsulation efficiency, drug release rate, and the morphology. The characterization methods in encapsulation studies are briefly explained below.

2.4.4.1 Preparation of Calibration Curve

Calibration curve can provide information on the relationship between drug absorption and drug concentration. The concentration can be measured with UV-Vis spectrophotometer or high-performance liquid chromatography (HPLC). Furthermore, the drug concentration in encapsulation efficiency and release studies can be calculated based on the calibration curve for the particular drug. Drug concentration serves as dependent variable while the absorbance serves as independent variable (Hsu & Chen, 2010).

2.4.4.2 Encapsulation Efficiency

The encapsulation efficiency can be determined by separating the encapsulated drug (within the carrier) and the free drug in the formulation. Based on previous literature, several techniques of separation have been introduced which include the mini-column centrifugation method where the analysis parameter make use of the difference in size of the encapsulated drug and the free drug. The undiluted suspension was applied dropwise on top of the sephadex gel column and the column is then centrifuged to force sedimentation of the void volume containing the drug carrier into the centrifuge tube (Fry *et al.*, 1978; Padamwar & Pokharkar, 2006).

Moreover, dialysis membrane with an appropriate cut-off method can be applied. The diluted vesicle suspension is dialysed against a buffer solution for two hours (Berger *et al.*, 2001). Ultrafiltration method using centrifugal devices can improve the storage stability from leakage and other disruptive conditions that affect the retention of encapsulant (Ezzati Nazhad Dolatabadi *et al.*, 2014). Other method that can also be applied to determine encapsulation efficiency is HPLC. In this method, the ratio of the un-encapsulated peak area to that of a reference standard at the same initial concentration is analyzed. Typically, HPLC method can be applied if the drug carrier has not undergoes purification analysis such as size exclusion chromatography (SEC) and detergent dialysis during its preparation (Singh *et al.*, 2005; Danoff *et al.*, 2007; Laouini *et al.*, 2012).

In this work, ultracentrifugation method was selected as it is the simplest and fastest method to separate drug loaded vesicles from supernatant. The supernatant and sediments can be observed in the tube after centrifugation at certain speed rate such as 5000 rpm, 15000 rpm, and so on (Laouini *et al.*, 2012). The spectrophotometry techniques that can be employed in quantification of the encapsulation efficiency are UV-Vis spectroscopy, fluorescence spectroscopy, enzyme-based methods, and electrochemical techniques.

2.4.4.3 Size and Zeta Potential

The carriers particle size is important in determining the target and biodistribution of drug, the route, and the drug release rate (Dhand *et al.*, 2014). For example, particles size of less than 10 nm can be simply removed by excretion through the kidneys, while large particles size of more than 150 nm will be eliminated by the mononuclear phagocyte system (MPS). It has been revealed that drug carriers with 100–150 nm in size could stay in the blood circulation for a longer period of time. The particles distributions are described using polydispersity index (PD1). The PDI reflects the nanoparticle stability and uniformity of distributed particles. High PDI value indicates the presence of

aggregation that lowers the stability of the nanoparticles due to inhomogeneity. On the other hand, low value of PDI indicates a homogeneous, highly stable, and uniform size distribution of nanoparticles (Popovska *et al.*, 2013; Masarudin *et al.*, 2015). The particle size and PDI of drug carriers are usually measured by DLS. Other than the information on the particle size, DLS also can be used to study the interaction of the drug carrier with its environment. The interaction is called zeta potential. In general, zeta potential is determined from the interference of the scattered light by particles (Abhish & Savkare, 2015). If large negative or positive value of zeta potential was discovered, it indicates that the suspensions have strong repulsive interactions. On the other hand, low zeta potential value indicates high possibility of coagulation to occur (Laouini *et al.*, 2012).

2.4.4.4 Morphological Analysis

There are a few techniques used in morphological analysis such as the transmission electron microscopy (TEM), scanning electron microscopy (SEM), and field emission scanning electron microscopy (FESEM). These analytical techniques are used to visualise the morphology and shape of the drug carriers with encapsulated drug whether they are spherical, discrete, abundant or uniformly distributed. MLV and large LUV can be visualised using cryogenic transmission electron microscopy (Cryo-TEM). The roughness of the drug carriers can also be determined from this technique (Saritha, 2015). Normally, TEM is used to identify micellar and vesicular dispersion as they contain high amount of water. FESEM is selected among all of the equipment since it has the advantage of visualising high-resolution image of drug loaded nanocarriers in various composition ratio. This technique sensitivity is contributed by its intensive and monochromatic beam (Zhang & Feng, 2006).

2.4.4.5 *In vitro* Release Studies

Drug release is the process in which the drug is involved in pharmacological actions such as absorption, distribution, and excretion. The importance of drug release is to control the bioavailability and the therapeutic efficacy of drug. There are numerous circumstances in drug release such as immediate release, modified release, delayed release, extended release, and controlled release.

Various methods of drug release have been introduced including; sample and separate method, continuous flow method, dialysis membrane method followed by voltammetry and turbidimetry. For sample and separate method, it requires a simple set-up which enables a direct measurement of drug release however the sampling process is impractical. The small size of the nanoparticulate drug (<10μm) molecules may cause filter clogging and adsorption of drug to filter (Kim *et al.*, 1997). The continuous flow method introduced a straightforward sampling but the set-up preparation is time-consuming. Maintaining a constant flow rate is a challenge for this method that may result in incomplete drug release (D'Souza & DeLuca, 2006). In dialysis membrane method, both the set-up and the sampling at periodic intervals are more straightforward. The most common system used in this method is dialysis bag where the formulation suspension is introduced into a dialysis bag that is place in buffer solution. The dialysis bag must be sealed properly to avoid leakage. Among all the mentioned methods above, dialysis bag method was selected in this research due to the simplicity of its set up preparation and its applicability for vesicles.

2.5 Concluding Remarks

In this studies, diorganotin(IV) dithiocarbamates complexes were synthesized. The highest cytotoxic activity of diorganotin(IV) dithiocarbamates complex against all tested cancer cell lines was selected for encapsulation studies. Thin film hydration method was

chosen to prepare mixed vesicles of cationic/non-ionic as a drug carrier. Intravenous injection as administration of drugs and DLS was used to measure size and zeta potential of vesicles encapsulated with drug. FESEM for morphological analysis and dialysis bag method for *in vitro* drug release studies.

CHAPTER 3: METHODOLOGY

3.1 General Introduction

This chapter will introduce the materials and methods used in this research. The experimental procedures of synthesized dithiocarbamate ligands and its diorganotin(IV) dithiocarbamate complexes as well as preparation method for encapsulation studies of dimethyltin(IV)chloride *N,N*-diethyldithiocarbamate (C7) will also be discussed in this chapter. Basically, the flow chart below (**Figure 3.1**) describes the overview of this research.

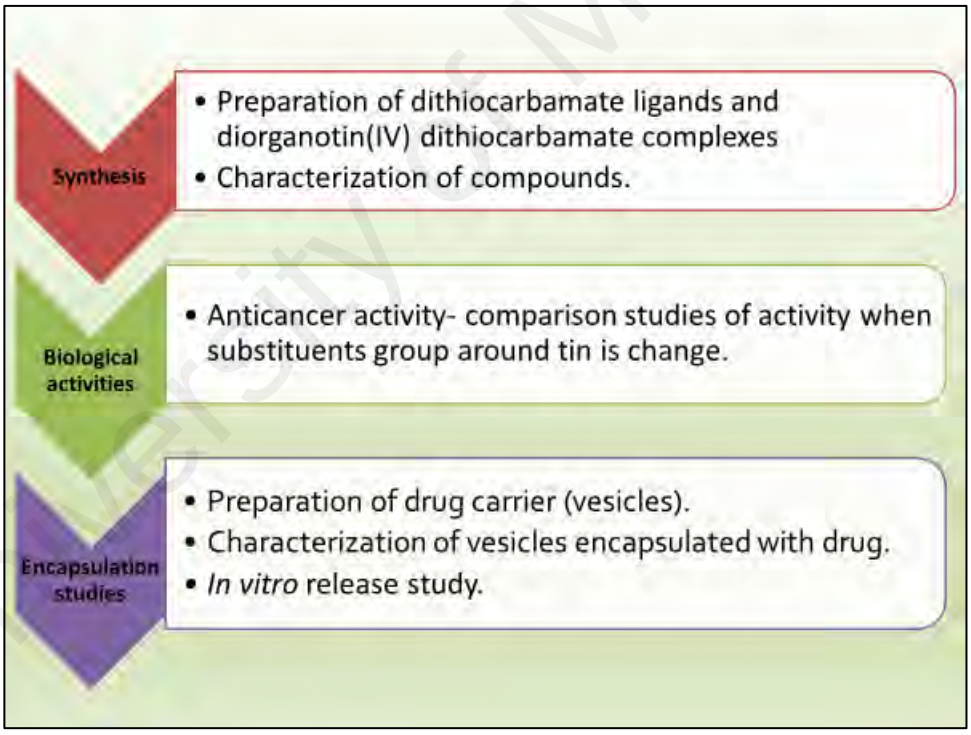

Figure 3.1: Overview of research.

3.2 Materials

The commercially available reagent-grade chemicals used in the preparations of the ligands and complexes are as follow; *N*-methylaniline, morpholine, *N,N*-phenyl piperazine, sodium *N,N*-diethyldithiocarbamate trihydrate, *N,N*-dimethyldithiocarbamate, sodium hydroxide, and dimethyltin(IV) dichloride. All chemicals were purchased from Merck and TCI Mark. The chemicals used for encapsulation part were phosphate buffer saline (PBS), dodecyl trimethyl ammonium bromide (DTAB) purchased from Merck; and hexyldecyl lactoside was obtained from own production (Hussen, 2010; Hussen, 2012). All solvents used in the reactions were procured commercially and used without further purification. The solvents used were ethanol, methanol, chloroform, acetonitrile, and acetic acid.

3.3 General Synthesis

The dithiocarbamate ligands were prepared from substituted amines with carbon disulphide following the procedure from Khan *et al*. (2015) without any modification (Zhang *et al.*, 2001; Manohar *et al.*, 2013). The diorganotin(IV) complexes were prepared from dithiocarbamate ligands with organotin starting materials. Ten mixed diorganotin(IV) dithiocarbamate complexes; dimethyltin(IV) *bis*(dithiocarbamate) series and dimethyltin(IV) chloride dithiocarbamate series were successfully synthesized.

3.3.1 Synthesis of Ligands

Ethanolic solution of 5 mmol secondary amine (*N*-methylaniline or *N*-morpholine or *N,N*-phenylpiperazine) was mixed with 5 M of sodium hydroxide (NaOH) in a conical flask. Then, 5 mmol of carbon disulphide was added dropwise. The reaction mixture was then stirred at low temperature (by immersion in ice water) for 30 minutes and the stirring was continued for another 1 hour 30 minutes at room temperature to produce sodium *N*-phenyl-*N*-methyldithiocarbamate (L3), sodium morpholinodithiocarbamate (L4), and

sodium *N,N*-phenylpiperazine dithiocarbamate (L5) ligands. Two commercially available ligands that were used in this research are sodium *N,N*-dimethyldithiocarbamate (L1) and sodium *N,N*-diethyldithiocarbamate trihydrate (L2). The reaction schemes for the preparation of the dithiocarbamate ligands for L1, L2, L3, L4, and L5 and their general structures are shown in **Scheme 3.1**. The substituents for the group R_1 and R_2 are as follow: **L1**; R_1 and $R_2 = CH_3$, **L2**; R_1 and $R_2 = CH_2CH_3$, **L3**; $R_1 = CH_3$, R_2 = phenyl (Ph), **L4**; R_1 and R_2 = morpholine, **L5**; R_1 and R_2 = Phenyl-*N*-cyclobutane.

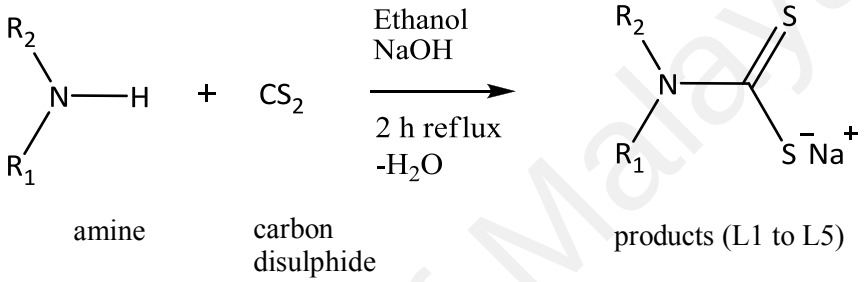

Scheme 3.1: General reaction of dithiocarbamate ligand.

3.3.2 Synthesis of Diorganotin(IV) Dithiocarbamate Series

In this study, two diorganotin(IV) dithiocarbamate series were successfully synthesized. The first series is based on the dimethyltin(IV) *bis*(dithiocarbamate) series. They were prepared in 2:1 molar ratio of dithiocarbamate ligands that had been previously prepared (see **Section 3.3.1**) to dimethyltin(IV) dichloride. The reactions will produce complexes which later will be known as C1, C2, C3, C4, and C5. On the other hand, the second series are based on the dimethyltin(IV)chloride dithiocarbamate and were prepared in 1:1 molar ratio of dithiocarbamate ligands to dimethyltin(IV) dichloride. The products are named as C6, C7, C8, C9, and C10. The general reaction scheme of dimethyltin(IV) *bis*(dithiocarbamate) series and dimethyltin(IV)chloride dithiocarbamate series are shown in **Scheme 3.2** and **Scheme 3.3** respectively.

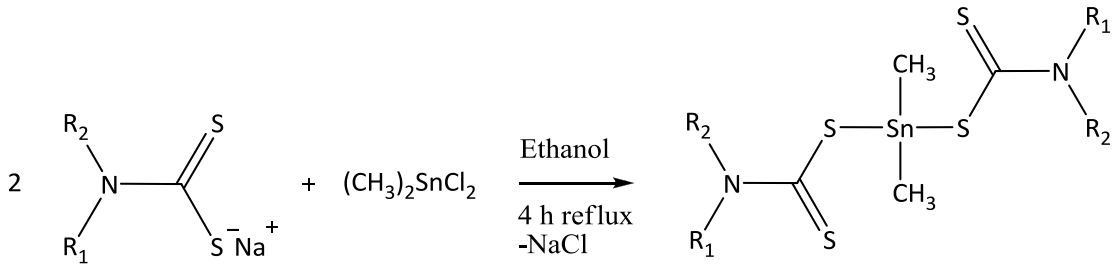

L1 or L2 or
L3 or L4 or L5

C1 or C2 or C3 or C4 or C5

Scheme 3.2: General reaction to produce dimethyltin(IV) *bis*(dithiocarbamate) series.

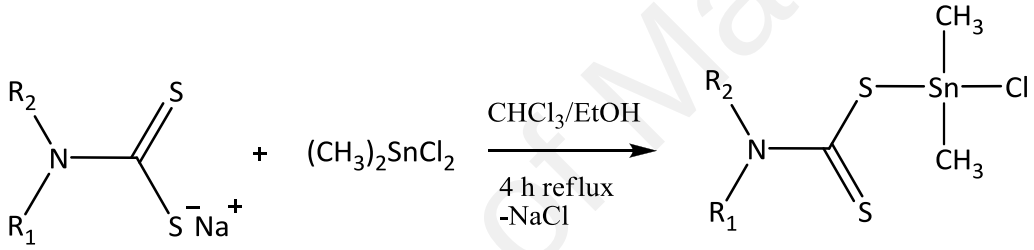

L1 or L2 or
L3 or L4 or L5

C6 or C7 or C8 or C9 or C10

Scheme 3.3: General reaction to produce dimethyltin(IV)chloride dithiocarbamate series.

The C1, C2, C3, C4, and C5 complexes were prepared by following the procedure given in the literature (Honda *et al.*, 1968; Khan *et al.*, 2008) where solution of dimethyltin(IV) dichloride (1 mmol) was added to the respective dithiocarbamate ligands (L1-L5) (2 mmol) in suitable solvent (ethanol or methanol) depending on their solubility. The mixture was then refluxed for 4 hours. The resulting mixture will be precipitated out upon cooling to room temperature. The precipitate was then filtered and recrystallised in ethanol (C1, C2, and C4), methanol (C3), and chloroform (C5).

Complexes C6, C7, C8, C9, and C10 were prepared by following an established procedure by (Honda *et al.*, 1968) with a modification where 10 mmol of

dimethyltin(IV) dichloride was added to each of the 10 mmol dithiocarbamate ligands (L1-L5) in 1:1 volume ratio mixture of mixed solvent of $CHCl_3$/EtOH. The mixture was refluxed for 4 hours and then left to stir at room temperature for a few more hours until a change in the colour of the solution was observed. The resulting mixture was then concentrated using rotary evaporator. The precipitate formed upon cooling to room temperature was filtered out and the product was recrystallised in 1:1 volume ration mixture of mixed solvents $CHCl_3$/EtOH.

3.4 Characterization Methods

For structural confirmation of the ligands and the corresponding organotin complexes, instrumentation tools such as FTIR, ^{1}H-NMR, and ^{13}C-NMR spectroscopies were utilized. For crystalline compounds, single crystal X-ray crystallography was carried out to determine its structures. Electronic properties of the compounds were studied using UV-Vis spectroscopy. Determination of percentage composition C, H, N, and S in complexes were carried out using CHNS elemental analyzer.

The melting points of the ligands and its organotin complexes were determined by Melt-Temp II melting point apparatus. The infrared spectroscopic analysis of the compounds was characterized by Perkin Elmer Spectrum 400 FT-IR/ FT-FIR Spectrometer. ^{1}H-NMR and ^{13}C-NMR spectra were recorded on a JEOL ECA-400 MHz spectrometer and AVN Bruker-400 MHz spectrometer. UV-Vis spectra were recorded on UV-1650PC SHIMADZU UV-Vis Spectrophotometer and UV-2500 SHIMADZU UV-Vis Spectrophotometer. The elemental analysis of carbon, hydrogen, nitrogen, and sulphur were determined using Thermofischer Scientific FlashSMART CHNS/O analyser. Intensity data for X-ray crystallography were measured at 100 K on Agilent SuperNova, Dual, Cu at zero, AtlasS2 diffractometer fitted with Cu $K\alpha$ radiation so that θ_{max} = 76.8°. Data processing and absorption correction were completed with CrysAlis

PRO. The structures were solved by direct method with SHELXS (Sheldrick, 2008) and refinement on F^2 was by means of SHELXL2014 (Sheldrick, 2015). The molecular structure was drawn with ORTEP-3 for Windows (Farrugia, 2012). The following sub topics elaborated on the details of the experimental work.

3.5 Biological Activities of Ligands and Complexes

The dithiocarbamate ligands and its corresponding organotin complexes have been evaluated against three carcinoma cell lines namely; human lung carcinoma cell line (A549), human prostate cancer cell line (PC-3), and human breast cancer cell line (MCF-7). The synthesized compounds were screened using 3-(4,5-dimethylthiazol-2-yl)-2,5-diphenyltetrazolium bromide (MTT) for cytotoxicity assay. In this research, the MTT assay was conducted based on the protocol used by Mosmann (1983) with some modifications. For this procedure, cells were preserved in basic culture medium and supplied with 10% fetal bovine serum and 2% penicillin/streptomycin. The cells were then cultured and seeded in a 96-well microtiter plate (Nunc, Germany) at a concentration of 7000 cells per well and incubated in CO_2 incubator at 37 °C. After 24 hours, the cells were treated with the samples and left to incubate for 72 hours. The samples were then diluted with dimethylsulfoxide (DMSO) until they achieved 0.5% (v/v) concentration in each well. At the end of the incubation period, 20 µL of MTT working solution (5 mg/mL) was added into each well and the 96-well microtiter plate was incubated for another 3 hours at 37 °C. The solution was then gently aspirated from each well and 200 µL of DMSO was added to solubilise the purple formazan crystals. The absorbance values were determined using a Multiskan GO micro plate spectrophotometer (Thermo Fisher Scientific Inc., Waltham, MA, USA) at 570 nm with 650 nm as the reference wavelength. IC_{50} value was used to determine the cytotoxic activity of the sample where concentration of the test sample that causes 50% inhibition of cell growth (Lim *et al.*, 2014; Lee *et al.*, 2015).

3.6 Encapsulation Studies

Dimethyltin(IV)chloride *N,N*-diethyldithiocarbamate (C7) was selected for further studies in encapsulation. In order to determine the concentration of complex C7 in the samples, a calibration curve of C7 drug was prepared in advance. Then, the drug carrier (mixed vesicles of cationic/non-ionic surfactant) was prepared by thin film hydration method. The characterization methods involved for vesicles are size distribution, zeta potential, and polydispersity index (PDI). Furthermore, the encapsulation efficiency of vesicles was determined by ultracentrifugation method and the drug release studies were also investigated. Finally, the morphology and shape of the vesicles with encapsulated drug were visualised using FESEM. The experimental procedure of each characterization method is elaborated further below.

3.6.1 Preparation of Calibration Curve of Dimethyltin(IV)chloride *N,N*-diethyldithiocarbamate, C7

Various concentrations of dimethyltin(IV)chloride *N,N*-diethyldithiocarbamate ranging from 0.0005 mM to 0.03 mM were prepared in two different mediums (PBS and acetic acid). The absorbances in PBS and acetic acid were measured using UV-Vis spectrophotometer at 201 nm 253 nm respectively. Plots of absorbance versus concentration were constructed based on the measurements. The reference wavelength was selected based on the optimum peak shown at a particular solvent.

3.6.2 Preparation of Drug Carriers

The vesicles were prepared by thin film hydration method as shown in **Figure 3.2**. 1:1:10 mole ratio of dodecyl trimethyl ammonium bromide (DTAB) surfactant: carbohydrate surfactant: C7 drug were dissolved in a mixture of acetic acid and ethanol solvent. Then, the organic solvent was eliminated under reduced pressure using rotary vacuum at 50 °C for 1 hour to form a thin film as shown in **Figure 3.3**. The film was

hydrated by adding 25 mL of phosphate buffer saline (PBS, pH 7.4) followed by agitation for 1 hour to form vesicles suspension.

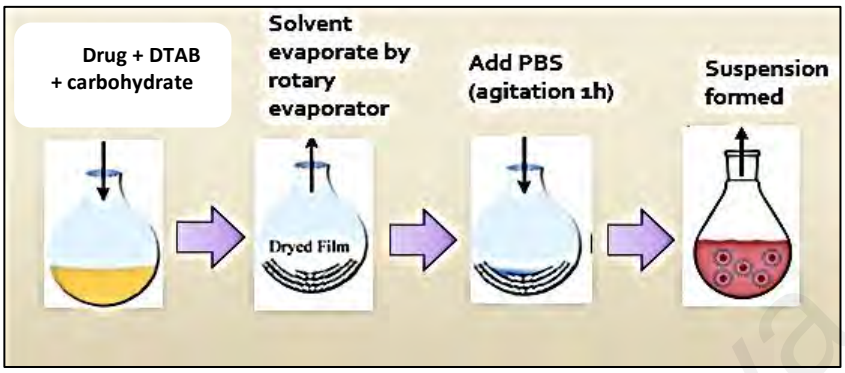

Figure 3.2: Schematic representations of vesicles preparation.
(adapted from (Ai *et al.*, 2014; Moghassemi & Hadjizadeh, 2014))

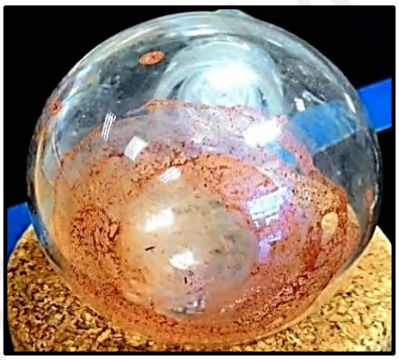

Figure 3.3: Formation of thin film.

3.6.3 Encapsulation Efficiency by Ultracentrifugation

The percentage of encapsulation efficiency was determined by ultracentrifugation method using Velocity 18R Refrigerated Centrifuge. The vesicles solution as prepared in **Section 3.5.2** was centrifuged at 15000 rpm for 30 minutes. The absorbance of the supernatant was measured at 201 nm. The sediment later then disrupted with acetic acid and the absorbance was measured again at 253 nm.

The amount of drug present was calculated from the calibration curves of concentration versus absorbance. The percentage of encapsulation efficiency (*%EE*) was calculated as followed:

$$EE\ (\%)\ =\ (\frac{T-C}{T})\ x\ 100, \qquad \text{(Equation 1)}$$

where *T* is the total amount of drug used and *C* is the amount of free drug present in the aqueous phase of the supernatant (Yassin *et al.*, 2010; Bruckman *et al.*, 2016). The percentage of drug loading (*DL%*) was calculated as followed:

$$DL\ (\%)\ =\ (\frac{T-C}{[T+\ (S-C)]})\ x\ 100\%, \qquad \text{(Equation 2)}$$

where *T* is the total amount of drug used, *C* is the amount of free drug present in the aqueous phase of the supernatant, and *S* is the total amount of surfactant use (Yassin *et al.*, 2010).

3.6.4 Drug Release Studies

The release of C7 was investigated using dialysis tubing method in buffer solution. 5 ml of encapsulated C7 was sealed into membrane dialysis tube and immersed in the release medium (Phosphate Buffer Saline, PBS) at 37 °C. The buffer solution temperature was maintained at 37 °C using water bath. The volume of the medium was kept constant throughout the test with the constant addition of 1 mL fresh medium upon 1 mL collection of the medium for absorbance measurement. The release medium was collected at 0, 1, 2, 4, 6, 8 hours followed by predetermined day up to 60 days. The amount of the encapsulated drug was calculated based on the calibration curve (Zhao *et al.*, 2016).

3.6.5 Size and Zeta Potential

The size and zeta potential of the vesicle loaded C7 was measured by filtered through a polycarbonate membrane with pore size 0.2 μm to remove any macro particles in the solution. Subsequently, the solution was measured with dynamic light scattering (DLS). The measurement was carried out at 25 °C using Malvern Zetasizer at the scattering angle of 173° using the refractive index and viscosity of water as the dispersant.

3.6.6 Morphological Analysis by FESEM

A few drops of vesicles suspension were placed on polycarbonate membrane and left to air dried at room temperature. The dried vesicle loaded C7 was then viewed under FESEM at 1 kV accelerating voltage.

3.7 Concluding Remarks

In this work, the characterization methods that were used to determine the structural features for dithiocarbamate ligands and diorganotin(IV) dithiocarbamate complexes are IR, NMR comprising ^{1}H-NMR and ^{13}C-NMR, UV-Vis spectroscopy, and CHNS elemental analyzer. In addition, X-ray crystallography was used for three-dimensional structure determinations. These methods are applicable to determine and verified the structure, purity, and coordination structure of the synthesized compounds. For biological activities, MTT assay method was applied to analyze anticancer activities of ligands and complexes against three carcinoma cell lines; A549, PC-3, and MCF-7. In encapsulation studies, thin film hydration method was used to prepare vesicles. Then, the vesicles loaded C7 were characterized using DLS to measure its size, zeta potential, and PDI. The percentage encapsulation efficiency was determined by ultracentrifugation method. Dialysis of tubing method was utilized to investigate the release of C7 drug and FESEM was applied to visualize morphology and shape of vesicles loaded C7.

CHAPTER 4: RESULTS AND DISCUSSION

4.1 General Introduction

The characterization of dithiocarbamate ligands and its diorganotin(IV) dithiocarbamate complexes include the FTIR spectroscopy, NMR spectroscopy, UV-Vis spectroscopy, CHNS elemental analysis and X-ray crystallography will be presented and discussed in this chapter. The data for the encapsulation studies including the particle size distribution, zeta potential, polydispersity index (PDI), percentage of encapsulation efficiency, drug loading, drug release rate, and morphological analysis will be also addressed.

4.2 Synthesis of Dithiocarbamate Ligands and Dimethyltin(IV) Dithiocarbamate

The dithiocarbamate ligands of L1 and L2 were used as received but the physical properties such as the melting points, FTIR, NMR, and the UV-Vis were carried out. The dithiocarbamate ligands of L3, L4, and L5 were prepared as sodium salts from the reaction of amine and carbon disulphide with sodium hydroxide in ethanol. The dithiocarbamate ligands were light yellow in colour for L1, yellowish brown in colour for L3 and white for L2, L4, and L5. The yield for most of the synthesized compounds were in agreement with the percentage yield of diorganotin(IV) dithiocarbamate found in literatures at approximately 55%–80% percentage yield (Zia ur *et al.*, 2009; Khan *et al.*, 2015; Mohamad *et al.*, 2016). However, some of the synthesized compound gave lower yield due to the loss during evaporation, filtration and dissolution.

The adduct formation of the dithiocarbamate complexes were influenced by the movement of electrons to sulphur atoms of dithiocarbamate ligands due to the mesomeric effect of -NR_2 groups, thus, resulting in the donation of electrons from the sulphur atoms

to the nonbonding molecular orbital of the tin atom to form a coordination bond S→Sn to stabilize the overall structure (Xiong *et al.*, 1997; Ekennia *et al.*, 2015). The stability and physicochemical properties of a metal complex depend on the properties of the R-group in the $–NR_2$ moiety. Dithiocarbamate ligand has strong chelating ability to form stable complexes with most of the elements. This ability is due to the presence of anionic CS_2^- moiety that can form various binding modes such as monodentate, bidentate or bridging upon complexation. Since diorganotin halides are relatively strong Lewis acid, it can form stable complexes with dithiocarbamate ligands (Tiekink, 2008).

4.3 Characterization Data of Ligands and Complexes

The structure of the dithiocarbamate ligands and its diorganotin(IV) complexes are shown in **Figure 4.1-Figure 4.15**. Their substituents are shown in **Table 4.1**. The physical appearance, percentage yield, melting points, NMR assignment, maximum wavelength absorbance, and CHNS analyzer data for some of the compounds are presented in page 43–50.

Table 4.1: Substituents of ligands and complexes.

Compounds	R group
L1, C1, C6	$R_1=R_2=CH_3$
L2, C2, C7	$R_1=R_2=CH_2CH_3$
L3, C3, C8	$R_1=CH_3$; $R_2=$ 
L4, C4, C9	$R_1=R_2=$ 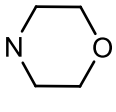
L5, C5, C10	$R_1=R_2=$ 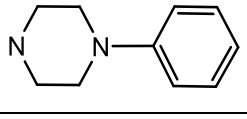

a) Dithiocarbamate Ligands

Sodium *N,N*-dimethyldithiocarbamate, L1

Colour: Light-yellow solid. Melting point: 115-118 ºC. Selected IR data (FTIR) cm^{-1}: 1489(m) ν(C=N), 969(s) ν(C=S). ^{1}H NMR (DMSO-d_6) δ (ppm): 3.49 (s, 6H, N–CH_3). ^{13}C NMR (DMSO-d_6) δ (ppm): 43.14 (N–CH_3), 192.68 (N–CS_2). UV(λ_{max}, nm): 215, 284. Molecular weight: 143.21 $gmol^{-1}$.

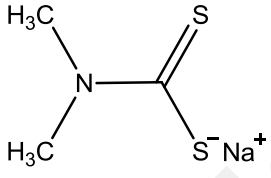

Figure 4.1: Structure of L1.

Sodium *N,N*-diethyldithiocarbamate trihydrate, L2

Colour: White solid. Melting point: 66-68 ºC. Selected IR data (FTIR) cm^{-1}: 1475(s) ν(C=N), 984(s) ν(C=S). ^{1}H NMR (DMSO-d_6) δ (ppm): 1.10-1.37 (m, 6H, CH_3), 3.96-3.97 (m, 4H, N−CH_2). ^{13}C NMR (DMSO-d_6) δ (ppm): 12.95 (CH_3), 42.15(N−CH_2), 193.19 (N–CS_2). UV(λ_{max}, nm): 264, 301. Molecular weight: 225.31 $gmol^{-1}$.

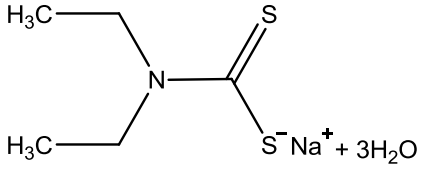

Figure 4.2: Structure of L2.

Sodium *N*-methyl-*N*-phenyldithiocarbamate, L3

Colour: Yellowish brown solid. Yield: 64%. Melting point: >360 ºC (decomposed). Selected IR data (FTIR) cm^{-1}: 1489(s) ν(C=N), 956(s) ν(C=S). ^{1}H NMR (DMSO-d_6) δ (ppm): 3.72 (m, 3H, N–CH_3), 7.47-7.56 (m, 5H, N–C_6H_4). ^{13}C NMR (DMSO-d_6) δ (ppm):

45.87(N−CH_3), 124.95, 127.24, 127.47, 150.71 (C aromatic), 196.12 (N−CS_2). UV(λ_{max}, nm): 206, 285. Molecular weight: 205.28 $gmol^{-1}$.

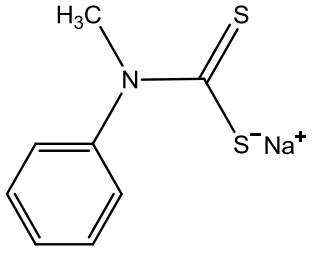

Figure 4.3: Structure of L3.

Sodium morpholinodithiocarbamate, L4

Colour: White solid. Yield: 54%. Melting point: 266 ºC (decomposed). Selected IR data (FTIR) cm^{-1}: 1459(s) ν(C=N), 975(s) ν(C=S). ^{1}H NMR (DMSO-d_6) δ (ppm): 3.49 (s, 4H, N−CH_2), 3.61 (s, 4H, CH_2−O). ^{13}C NMR (DMSO-d_6) δ (ppm): 51.93(N−CH_2), 66.22 (CH_2−O), 193.25 (N−CS_2). UV(λ_{max}, nm): 268. Molecular weight: 185.24 $gmol^{-1}$.

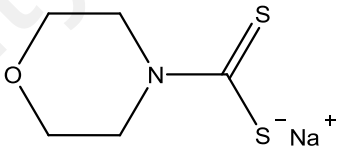

Figure 4.4: Structure of L4.

Sodium *N,N*-phenylpiperazinedithiocarbamate, L5

Colour: White solid. Yield: 56%. Melting point: 186-189 ºC. Selected IR data (FTIR) cm^{-1}: 1493(s) ν(C=N), 993(s) ν(C=S). ^{1}H NMR (DMSO-d_6) δ (ppm): 3.09-3.21 (m, 4H, N−CH_2), 4.44 (s, 4H, CH_2N−C_6H_4), 6.76-7.25 (m, 5H, C_6H_4). ^{13}C NMR (DMSO-d_6) δ (ppm): 43.35(N−CH_2), 46.16 (CH_2N−C_6H_4), 116.65, 120.76, 129.61, 150.48 (C aromatic), 212.48 (N−CS_2). UV(λ_{max}, nm): 257. Molecular weight: 260.35 $gmol^{-1}$.

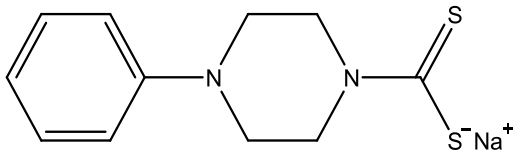

Figure 4.5: Structure of L5.

b) Dimethyltin(IV) *bis*(dithiocarbamate) Series

Dimethyltin(IV) *bis*(*N,N*-dimethyldithiocarbamate), C1

Colour: Light-yellow solid. Yield: 62%. Melting point: 197-199 ºC [Lit: 198-200 ºC]. Selected IR data (FTIR) cm^{-1}: 1536(m) ν(C=N), 2917(m) ν(C−H), 973(s) ν(C=S), 554(s) ν(Sn–C). ^{1}H NMR (DMSO-d_6) δ (ppm): 1.23(s, 6H, Sn–CH_3), 3.34(s, 12H, N−CH_3). ^{13}C NMR ($CDCl_3$) δ (ppm): 10.06(Sn–CH_3), 45.31(N−CH_3), 197.60 (N−CS_2). UV(λ_{max}, nm): 206, 247, 279. Molecular weight: 389.21 $gmol^{-1}$.

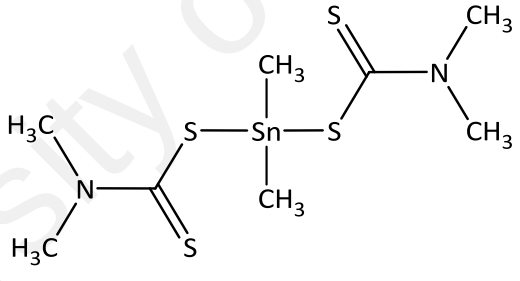

Figure 4.6: Structure of C1.

Dimethyltin(IV) *bis*(*N,N*-diethyldithiocarbamate), C2

Colour: White solid. Yield: 27%. Melting point: 133-138 ºC. Selected IR data (FTIR) cm^{-1}: 1486(s) ν(C=N), 2930(s) ν(C−H), 992(s) ν(C=S), 557(s) ν(Sn–C). ^{1}H NMR ($CDCl_3$) δ (ppm): 1.11(s, 6H, Sn–CH_3), 1.25-1.31 (m, 12H, CH_3), 3.81-3.87 (m, 8H, N−CH_2). ^{13}C NMR ($CDCl_3$) δ (ppm): 10.30 (Sn–CH_3), 29.86 (CH_3), 51.64 (N−CH_2), 197.35 (N−CS_2). UV(λ_{max}, nm): 259, 278. Molecular weight: 445.32 $gmol^{-1}$.

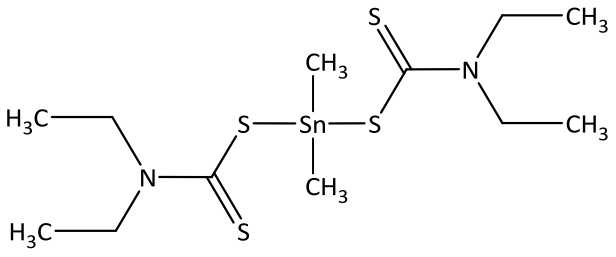

Figure 4.7: Structure of C2.

Dimethyltin(IV) *bis*(*N*-methyl-*N*-phenyldithiocarbamate), C3

Colour: Light-yellow. Yield: 51%. Melting point: 210-212 ºC. Selected IR(FTIR) cm^{-1}: 1489(s) ν(C=N), 2917(s) ν(C–H), 967(s) ν(C=S), 555(s) ν(Sn-C). ^{1}H NMR ($CDCl_3$) δ (ppm): 1.54 (s, 6H, Sn–CH_3), 3.70 (s, 6H, N–CH_3), 7.25-7.42 (m, 10H, N–C_6H_4). ^{13}C NMR ($CDCl_3$) δ (ppm): 14.16(Sn–CH_3), 40.59(N– CH_3), 126.02, 128.61, 130.02, 146.73(C aromatic), 202.70(N–CS_2). UV(λ_{max}, nm): 207, 251, 289. Elemental Anal. Calc. for $C_{18}H_{22}N_2S_4Sn$: C, 42.11; H, 4.32; N, 5.46; S, 24.98. Found: C, 42.21; H, 4.41; N, 5.83; S, 24.89. Molecular weight: 513.35 $gmol^{-1}$.

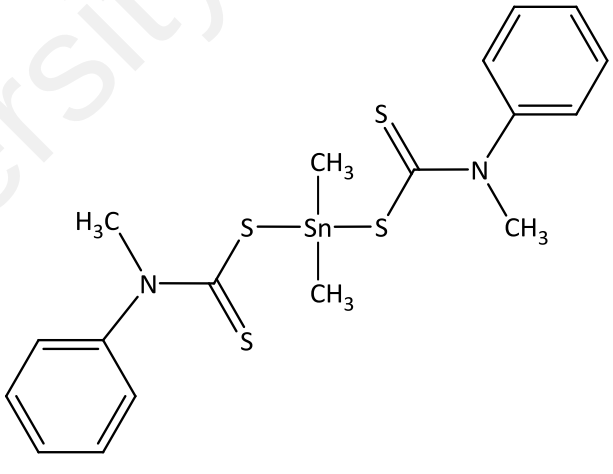

Figure 4.8: Structure of C3.

Dimethyltin(IV) *bis*(morpholinodithiocarbamate), C4

Colour: White. Yield: 57%. Melting point: 192-193 ºC. Selected IR(FTIR) cm^{-1}: 1464(s) ν(C=N), 2959(s) ν(C–H), 993(s) ν(C=S), 540(s) ν(Sn–C). ^{1}H NMR ($CDCl_3$) δ

(ppm): 1.54 (s, 6H, Sn-CH_3), 3.78 (s, 8H, N–CH_2), 4.11(s, 8H, CH_2–O). ^{13}C NMR ($CDCl_3$) δ (ppm): 15.61 (Sn–CH_3), 51.26(N–CH_2), 66.27(CH_2–O), 200.25(N–CS_2). UV(λ_{max}, nm): 263, 283. Molecular weight: 473.29 gmol^{-1}.

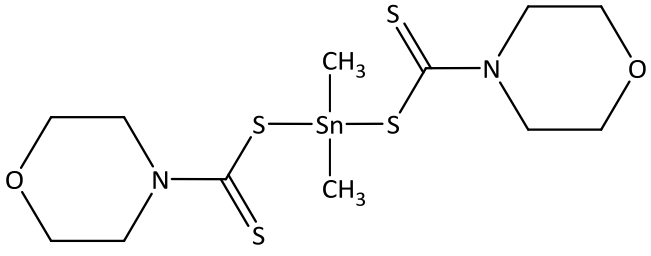

Figure 4.9: Structure of C4.

<u>Dimethyltin(IV) *bis*(*N,N*-phenylpiperazinedithiocarbamate), C5</u>

Colour: White. Yield: 52%. Melting point: 206-210 ºC. Selected IR(FTIR) cm^{-1}: 1503(s) ν(C ═N), 2898(m) ν(C− H), 1001(s) ν(C═S), 558(m) ν(Sn–C). ^{1}H NMR ($CDCl_3$) δ (ppm): 1.60 (s, 6H, Sn–CH_3), 3.21(s, 8H, N–CH_2), 4.17(s, 8H, CH_2N–C_6H_4), 6.83-7.23 (m, 10H, C_6H_4). ^{13}C NMR ($CDCl_3$) δ (ppm): 15.71(Sn–CH_3), 50.97(N–CH_2), 59.68(CH_2N− C_6H_4), 116.63, 120.80, 129.50, 150.44(C aromatic), 199.93(N− CS_2). UV(λ_{max}, nm): 256, 291. Molecular weight: 623.51 gmol^{-1}.

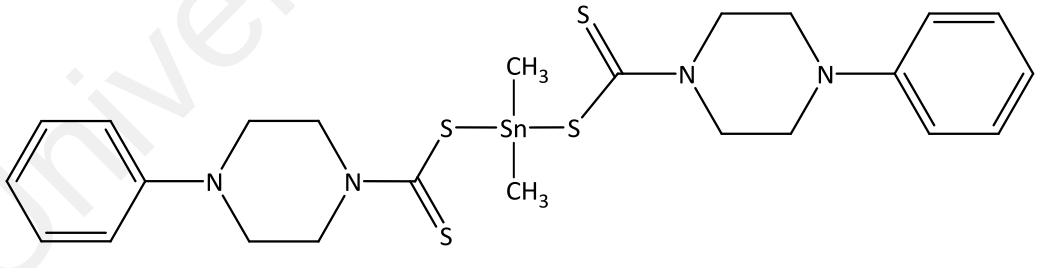

Figure 4.10: Structure of C5.

c) Dimethyltin(IV)chloride dithiocarbamate Series

Dimethyltin(IV)chloride *N,N*-dimethyldithiocarbamate, C6

Colour: White solid. Yield: 42%. Melting point: 135-136 ºC [Lit: 135-137 ºC]. Selected IR data (FTIR) cm^{-1}: 1536(s) ν(C═N), 2919(m) ν(C−H), 973(s) ν(C═S), 554(s) ν(Sn–C). ^{1}H NMR ($CDCl_3$) δ (ppm) : 1.29(s, 6H, Sn–CH_3), 3.41(s, 6H, N−CH_3). ^{13}C NMR ($CDCl_3$) δ (ppm): 10.11(Sn–CH_3), 45.36(N−CH_3), 197.54 (N−CS_2). UV(λ_{max}, nm): 206, 253, 280. Molecular weight: 304.45 $gmol^{-1}$.

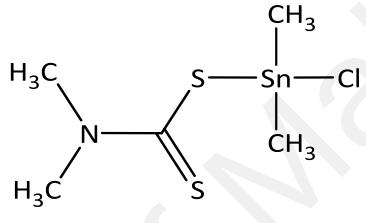

Figure 4.11: Structure of C6.

Dimethyltin(IV)chloride *N,N*-diethyldithiocarbamate, C7

Colour: White solid. Yield: 57%. Melting point: 84-86 ºC. Selected IR data (FTIR) cm^{-1}: 1512(s) ν(C═N), 2934(m) ν(C−H), 993(m) ν(C═S), 556(s) ν(Sn–C). ^{1}H NMR ($CDCl_3$) δ (ppm): 1.29(s, 6H, Sn-CH_3), 1.33-1.36 (m, 6H, CH_3), 3.73-3.79 (m, 4H, N−CH_2). ^{13}C NMR ($CDCl_3$) δ (ppm): 10.08 (Sn-CH_3), 12.14 (CH_3), 50.22 (N−CH_2), 195.76 (N−CS_2). UV(λ_{max}, nm): 256, 280. Elemental Anal. Calc. for $C_7H_{16}ClNS_2Sn$: C, 25.29; H, 4.85; N, 4.21; S, 19.29. Found: C, 24.92; H, 4.81; N, 4.55; S, 18.62. Molecular weight: 332.50 $gmol^{-1}$.

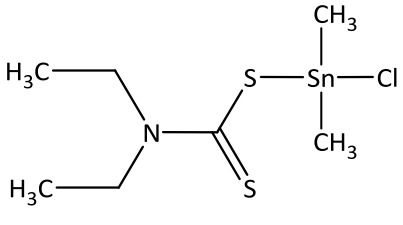

Figure 4.12: Structure of C7.

Dimethyltin(IV)chloride *N*-methyl-*N*-phenyldithiocarbamate, C8

Colour: Light-yellow solid. Yield: 28%. Melting point: 132-136 ºC. Selected IR(FTIR) cm^{-1}: 1490(m) ν(C=N), 2917(m) ν(C−H), 967(s) ν(C=S), 551(s) ν(Sn–C). ^{1}H NMR (DMSO-d_6) δ (ppm): 1.27 (s, 6H, Sn–CH_3), 3.62 (s, 3H, N−CH_3), 6.50-7.47 (m, 5H, N−C_6H_4). ^{13}C NMR (DMSO-d_6) δ (ppm): 29.83(Sn–CH_3), 46.70(N−CH_3), 125.83, 128.96, 129.71, 149.97(C- aromatic), 200.39(N−CS_2). UV(λ_{max}, nm): 205, 254, 288. Molecular weight: 366.52 $gmol^{-1}$.

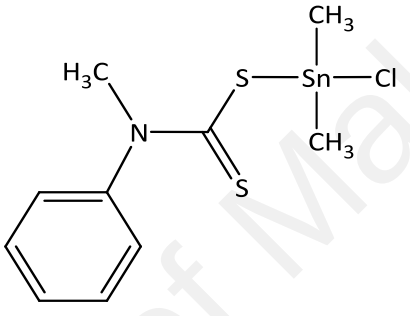

Figure 4.13: Structure of C8.

Dimethyltin(IV)chloride morpholinodithiocarbamate, C9

Colour: Light-yellow solid. Yield: 58%. Melting point: 145-148 ºC. Selected IR(FTIR) cm^{-1}: 1483(s) ν(C=N), 2917(m) ν(C−H), 998(s) ν(C=S), 541(s) ν(Sn–C). ^{1}H NMR ($CDCl_3$) δ (ppm): 1.30(s, 6H, Sn–CH_3), 3.79-3.81(m, 4H, N–CH_2), 3.96-3.98(m, 4H, CH_2−O). ^{13}C NMR ($CDCl_3$) δ (ppm): 10.29(Sn–CH_3), 51.63(N− CH_2), 66.02(CH_2 − O), 197.33(N–CS_2). UV(λ_{max}, nm): 258, 280. Molecular weight: 346.49 $gmol^{-1}$.

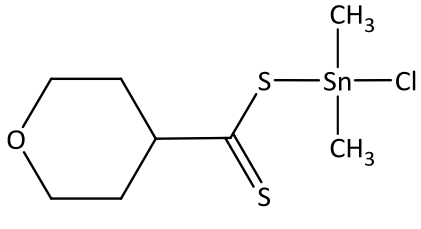

Figure 4.14: Structure of C9.

Dimethyltin(IV)chloride *N,N*-phenylpiperazinedithiocarbamate, C10

Colour: White solid. Yield: 43%. Melting point: 168-170 ºC. Selected IR(FTIR) cm^{-1}: 1500(s) ν(C═N), 2916(s) ν(C−H), 1002(s) ν(C═S), 554(s) ν(Sn–C). ^{1}H NMR ($CDCl_3$) δ (ppm): 1.60 (s, 6H, Sn–CH_3), 3.28-3.30(m, 4H, N−CH_2), 4.24-4.27(m, 4H, CH_2N−C_6H_4), 6.92-7.31 (m, 5H, C_6H_4). ^{13}C NMR ($CDCl_3$) δ (ppm): 10.28(Sn–CH_3), 29.88(N−CH_2), 48.97(CH_2N−C_6H_4), 116.86, 121.30, 129.58, 150.08(C aromatic), 196.90(N−CS_2). UV(λ_{max}, nm): 257, 292. Molecular weight: 421.60 $gmol^{-1}$.

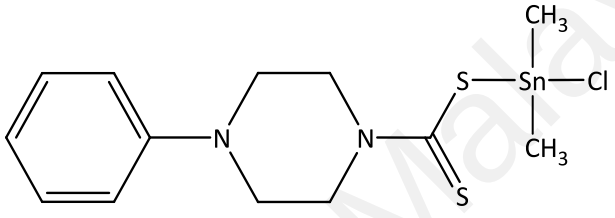

Figure 4.15: Structure of C10.

4.4 Fourier Transform Infrared (FTIR) Spectroscopy of Compounds

The FTIR spectroscopy analysis was conducted to observe the functional group and to discover the coordination compounds in the ligands and complexes. Infrared spectra of all compounds were recorded from 450 to 4000 cm^{-1}. The main vibrational stretching frequencies bands for ligands and diorganotin(IV) dithiocarbamate complexes were described in **Section 4.3**. The main stretching vibration found in the complexes are ν(C═N), ν(C═S), ν(Sn–C), and ν(C–H) while the stretching vibration in dithiocarbamate ligands are ν(C═N) and ν(C═S).

The ν(C═S) stretching frequencies for free ligands were predicted to be in the region of 940–1000 cm^{-1} (Baba *et al.*, 2011; Shaheen *et al.*, 2012). A sharp band was found in the region of 951–993 cm^{-1} in the ligands spectra which indicates the ν(C═S) bond. It shows the chelating nature of the dithiocarbamate ligands. In diorganotin complexes, most of the stretching vibration for ν(C═S) bond was found in the region of 966–1015

cm^{-1}. The shifted frequencies were clearly observed in the complexes spectra. This can be observed in the stretching vibration of **L4** at 975 cm^{-1} (shown in **Figure 4.16**) that shifted to 993 cm^{-1} and 998 cm^{-1} in **C4** and **C9.** The FTIR spectrum of **C9** is shown in **Figure 4.17**. These shifted values indicate a coordination of S→Sn bond.

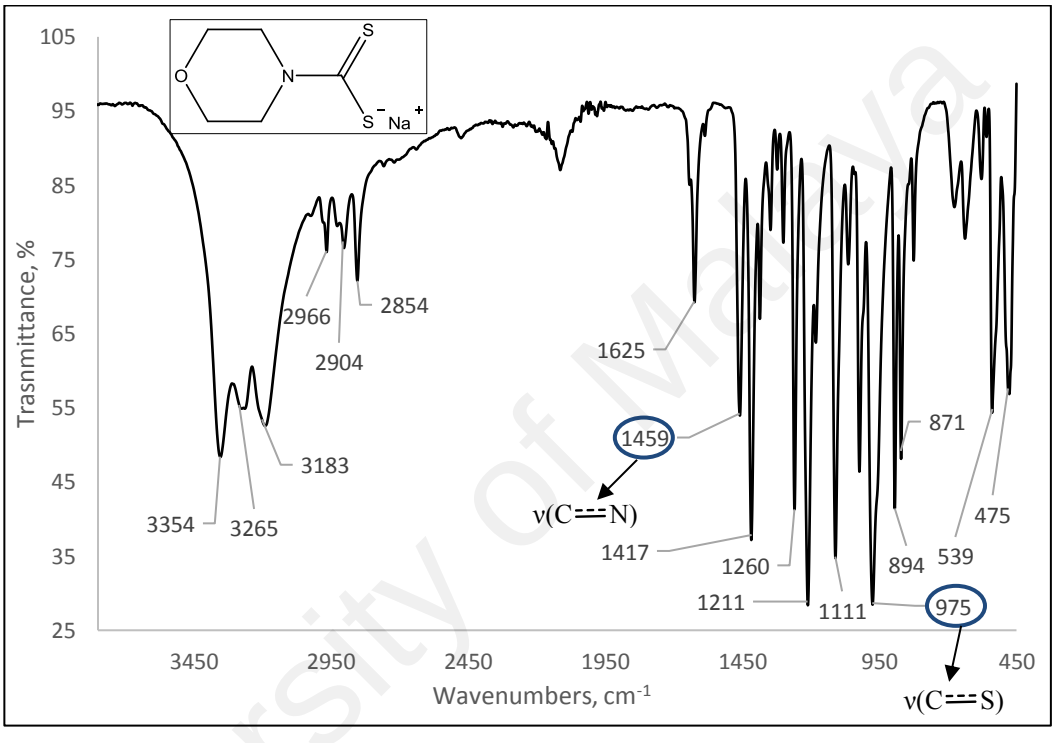

Figure 4.16: Infrared spectrum of L4.

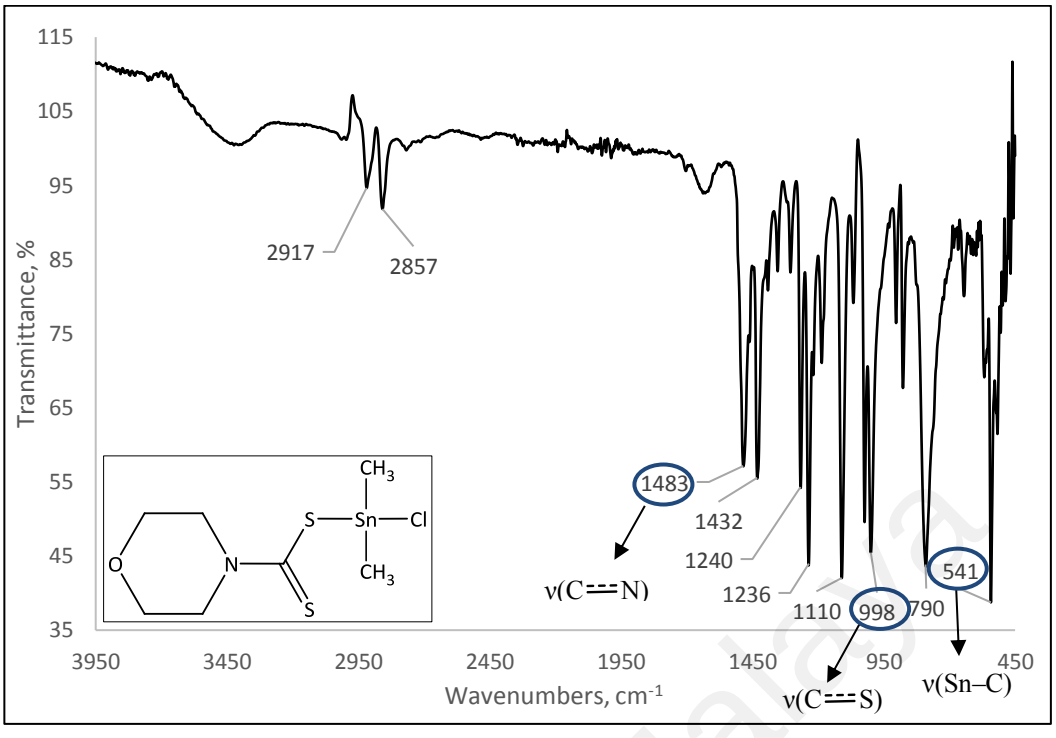

Figure 4.17: Infrared spectrum of C9.

All the dithiocarbamate ligands displayed the C═N stretching in 1459–1493 cm^{-1} region, which is within the range of previously reported C═N stretching in dithiocarbamate ligands (Ferreira *et al.*, 2012; Singh & Bhattacharya, 2012). It was suggested that thiouride band presence in the complexes spectra was manifested in the range of 1464–1536 cm^{-1} is a partial double bond character from the ν(C═N) bond vibration of the $S_2C–NR_2$ group. The ν(C═N) vibrations lie in the range of ν(C=N) double bond (approximately 1640–1690 cm^{-1}) and ν(C–N) single bond (approximately 1250–1360 cm^{-1}) (Awang *et al.*, 2010; Jayaraju *et al.*, 2012; Hussain *et al.*, 2016).

An increased in the frequencies of ν(C═N) stretching was observed between ligands complexes with the increase from 1459–1493 cm^{-1} in ligands to 1464–1536 cm^{-1} in complexes. As an example, the stretching of ν(C═N) in **L2** is 1475 cm^{-1} while the ν(C═N) stretching shifted towards higher frequencies in its corresponding complexes; **C2** and **C7** at 1486 cm^{-1} and 1512 cm^{-1}, respectively. These observations indicate an increasing character of $N–CS_2$ double bond (Ferreira *et al.*, 2014) as a results of bidentate bond formation between the dithiocarbamate and the Sn metal (Shaheen *et al.*, 2012).

The strong band found in the region of 2898–2934 cm^{-1} indicates the ν(C–H) stretching vibrations of methyl groups in the complexes (Khan *et al.*, 2015; Mohamad *et al.*, 2016). A sharp absorption band was manifested in lower frequency region of 540–557 cm^{-1} that was assigned to the ν(Sn–C) linkage, which points to the coordination of the complexes as observed in the appearance of this new band in the complex spectra and the absence of it in the ligands spectra. This ν(Sn–C) stretching frequency was within the range of previously reported diorganotin derivatives (Honda *et al.*, 1968; Zia ur *et al.*, 2011). The FTIR spectra for other ligands and complexes can be refer in appendix A.

4.5 Nuclear Magnetic Resonance (NMR) Spectroscopy

The deuterated solvents used in the NMR measurement for the dithiocarbamate ligands and its organotin complexes are DMSO-d_6 and $CDCl_3$ and the peak assignments were reported in **Section 4.3**. Tetramethylsilane was used as an internal standard for reference peak. ^{1}H-NMR and ^{13}C-NMR chemical shifts for the ligands and the diorganotin(IV) dithiocarbamate complexes were listed in **Section 4.3.**

4.5.1 ^{1}H-NMR

The multiplet resonance signals in the range 1.10–1.37 ppm for **L2** were assigned as methylene protons. The chemical shifts for the phenyl protons in **L3** and **L5** were found in the range 6.76–7.56 ppm. The (N−CH_2) and (CH_2−O) protons for ligand **L4** could be observed at 3.49 and 3.61 ppm, respectively at the slightly downfield position. This shift is due to the attachment of the methylene protons to the more electronegative elements which are oxygen and nitrogen (Zia ur *et al.*, 2009).

Similarly, the chemical shift of methylene protons in the diorganotin complexes was observed as a multiplets signal between 1.32–4.17 ppm. The presence of methylene protons could also be found between 3.07–4.17 ppm which is slightly deshielded than normal chemical shift of methylene protons. This is due to the attachment of the

methylene protons to the electronegative nitrogen atom in the dithiocarbamate ligands (Onwudiwe & Ajibade, 2010). The peaks at the chemical shift between δ 6.50–7.40 ppm for **C3, C5, C8,** and **C10** were assigned to the phenyl protons from the phenyl ring attached to the nitrogen atom. It appears at downfield region due to the electron donating effect of phenyl group. Furthermore, it was manifested as multiplet due to the overlapping proton signals in aromatic group (Awang *et al.*, 2011). The appearances of new signals for methyl group attached to the Sn atom were observed in the expected region of 1.18–1.30 ppm. This observation confirms the formation of complexes showing that Sn atom was chelated to the dithiocarbamate group (Jain *et al.*, 2012; Mohamad *et al.*, 2016). Overall, the chemical shift values for the aliphatic and aromatic protons of the complexes were found in the predicted region.

4.5.2 ^{13}C-NMR

The most significant ^{13}C-NMR chemical shift that can be used for identification in the characterization of the dithiocarbamate moieties is the chemical shift for CS_2. This shift was typically found in the range 185–220 ppm (Van Gaal *et al.*, 1979; Muthalib *et al.*, 2011). The chemical shifts of CS_2 in the synthesized ligands appeared in the range δ 192–197 ppm. Among the dithiocarbamate ligands, **L5** shows the highest chemical shift value of CS_2 at 212.48 ppm as the nitrogen inductively pulled the electron density out of the aryl ring.

On the other hand, the chemical shift of CS_2 in diorganotin complexes exhibit some shifted in the frequency in the range 197–200 ppm. This observation indicates that the ligand had coordinated to the Sn atom (Khan *et al.*, 2015). Chemical shift of CS_2 in **L2** ligand was observed at 193.19 ppm while its complexes **C2** and **C7** were observed at 197.34 ppm and 195.77 ppm, respectively. The high chemical shift value of CS_2 was probably due to an increase of π-bond order in the whole NCS_2 moiety (Ferreira *et al.*, 2012).

The chemical shifts of methylene carbons attached to nitrogen group appear at 41–52 ppm in ligands and complexes while the chemical shifts of aryl carbon that attached to nitrogen can be found between 115–151 ppm. These peaks were found in **C3** (shown in **Figure 4.18**), **C5, C8,** and **C10** due to the existence of phenyl ring in the complexes (Shaheen *et al.*, 2012). The chemical shift for the complexes shifted to deshielded region for all carbon resonance in comparison to free ligand due to the transfer of electron density from the ligand to the acceptor. The chemical shift for methyl group attached to the tin atom was in the expected region 10.06–29.83 ppm (Holeček *et al.*, 1986).

The ^{13}C-NMR chemical shifts show similarity with ^{1}H-NMR chemical shifts in the fact that they are affected by the presence of electronegative atom that results in the chemical shift to move towards the deshielded region. However, the electronegative effect is more prominent in ^{13}C-NMR than the ^{1}H-NMR. This observation might be due to the difference in specific anisotropic deshielding effects (Macomber, 1991). The ^{1}H-NMR and ^{13}C-NMR can be referred in appendix B and C.

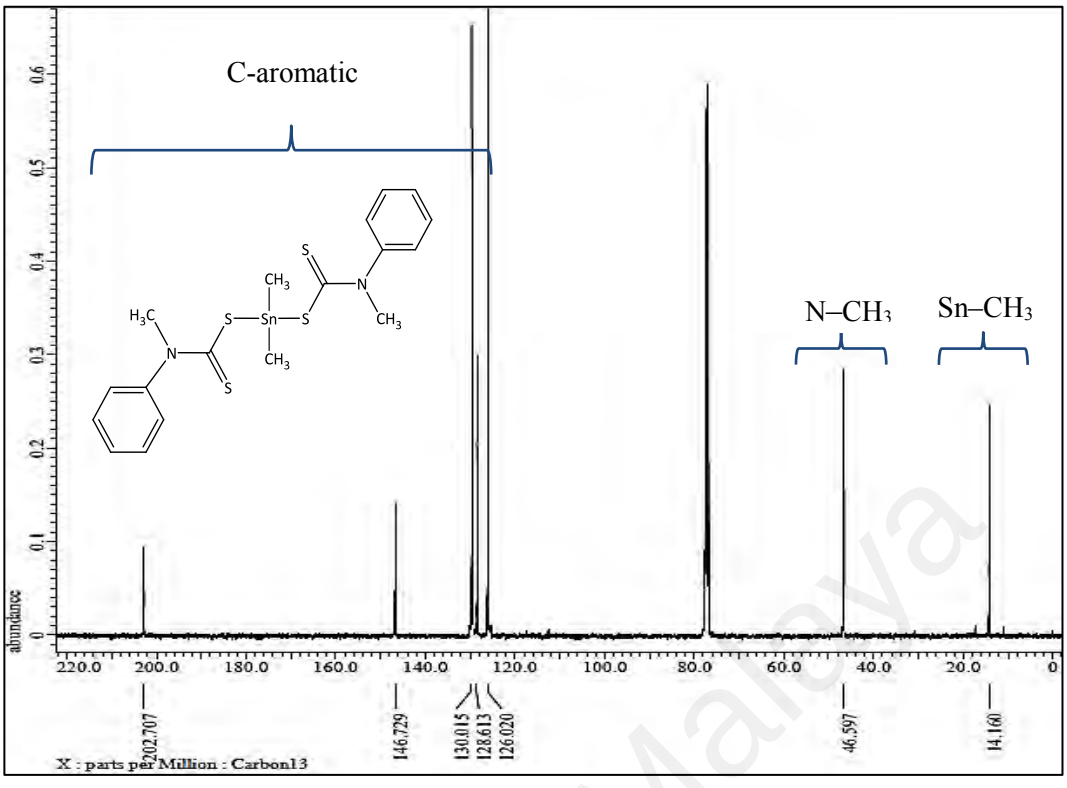

Figure 4.18: ^{13}C NMR spectrum of C3.

4.6 Carbon, Hydrogen, Nitrogen, and Sulphur (CHNS) Elemental Analysis

The percentage composition of C, H, N, and S of two new diorganotin(IV) complexes; dimethyltin(IV) *bis*(*N*-methyl-*N*-phenyldithiocarbamate) (**C3**) and dimethyltin(IV) chloride *N,N*-diethyldithiocarbamate (**C7**) were analyzed. Both complexes displayed less than 0.4% differences of experimental value from the theoretical value based on the predicted formula with exception for element S with the difference of 0.67% in compound **C7**. This difference was probably due to the difficulty of the compound to combust completely resulting in incomplete sulphur conversion and inaccurate outcome (Fadeeva *et al.*, 2008; Sainorudin *et al.*, 2015). The experimental data for the complexes as stated in **Section 4.3** were in fair agreement with the theoretical values. The data confirmed that both complexes were successfully synthesized in high purity (Farina *et al.*, 2002; Muthalib *et al.*, 2011).

4.7 X-ray Crystallography

The crystal of dimethyltin(IV) *bis*(morpholinodithiocarbamate), **C4** was grown by slow evaporation in ethanol at room temperature. The crystallographic and refinement details of **C4** is shown in **Table 4.3**. A skew-trapezoidal bipyramidal coordination geometry was observed in **Figure 4.19** where its octahedral coordination was due to the $R_2Sn(S_2CNRR')_2$ molecules (Tiekink, 2008). It occurs as the bidentate dithiocarbamate ligand chelate to the tin atom in an asymmetric mode as a consequence of 0.35Å distance difference between Sn—$S(3)_{long}$ and Sn—$S(1)_{short}$ bond length as shown in **Table 4.2**. This asymmetric Sn—S bond lengths suggests that disproportion of C—S bond lengths will produce longer Sn—S bond is associated with a short C—S bond length of approximately 0.05 Å (Mohamad *et al.*, 2017). The skew trapezoidal bipyramidal geometry of **C4** shows the coordination of two methyl groups that are bound to the tin atom over the long Sn—S which have an angle of 148.24° and 85.878° bound by sulphur at the tin atom as shown in **Table 4.2** (Yin & Xue, 2005).

Table 4.2: Selected geometric parameters (Å, °).

Atom	**Length /Å**
Sn-S1	2.542
Sn-S2	2.892
Sn-S3	2.564
Sn-S4	2.913
C1-S1	1.747
C1-S2	1.702
Atom	**Angle/°**
S1-Sn-S3	85.878
S2-Sn-S4	143.066
C11-Sn-C12	148.240

Table 4.3: Crystallographic and refinement details for dimethyltin(IV) *bis*(morpholinodithiocarbamate) (C4)[a].

Empirical formula	$C_{12}H_{22}N_2O_2S_4Sn$
Formula weight	473.24
Temperature/K	100
Crystal system	Monoclinic
Space group	$P2_1/n$
a/Å	10.1472 (1)
b/Å	13.6653 (1)
c/Å	13.8122 (1)
β / °	104.959 (1)
Volume / Å^3	1850.36 (3)
Z	4
Calculated density, D_x (Mgm^{-3})	1.699
F(000)	952
Absorption coefficient, μ / mm^{-1}	15.25
Crystal size (mm)	0.24 × 0.09 × 0.06
Reflections collected / unique	19588 / 3865(R_{int} = 0.031)
Refinement method	Full-matrix least-squares on F^2
$R[F^2 > 2\sigma(F^2)]$, $wR(F^2)$, S	0.024, 0.065, 1.07
Data / restraints / parameters	3865 / 0 / 192
Largest diff. peak and hole (eÅ^{-3})	0.45 and -0.50

[a] Computer programs: CrysAlis PRO (Rigaku Oxford Diffraction, 2015), SHELXS(Sheldrick, 2008), SHELXL2014 (Sheldrick, 2015), and ORTEP-3 for Windows (Farrugia, 2012).

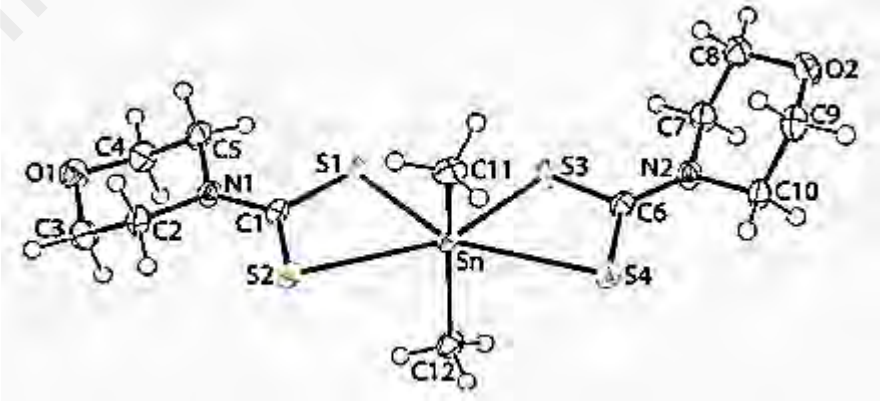

Figure 4.19: The molecular structure of coordination C4. Thermal ellipsoids at the 50% probability level.

4.8 Ultraviolet-visible (UV-Vis) Spectroscopy

UV-Vis spectroscopy analysis was carried out to observe the electronic transition of the synthesized ligands and complexes. It is important to confirm all the ligands and complexes were completely dissolved during the analysis as undissolved component may block the UV-Vis ray from passing through the solution (Sainorudin *et al.*, 2015). The wavelength used was in between 190 nm to 500 nm.

Typically, organotin(IV) dithiocarbamates will exhibit two bands. The two most important bands displayed were the (C=N) chromophore and the sulphur atoms containing lone pair. These two bands verified the formation of the complex. The electronic spectra of the dithiocarbamate ligands and their complexes were summarized in **Section 4.3**.

Intramolecular π–π^* transitions called the hypsochromic shift (blue shift) were present in the spectra of dithiocarbamate ligands and its complexes. This single strong absorption peak appeared in the region of 206 nm to 268 nm for ligands while in complexes this transition was observed in the region of 205 nm to 263 nm. This shifted is due to the chelating formation of NCS_2 with Sn. The bond formation was confirmed by the existence of (C=N) bands at this shorter wavelength (Husain *et al.*, 2009; Basirah *et al.*, 2013).

Furthermore, the existence of n–π^* transition corresponding to the bathochromic shift (red shift) were found in between 277 nm to 301 nm. The peak absorbance was slightly lower due to the stabilisation of non-bonding electron in sulphur. Hence, the observed peak implies the presence of lone pair electrons at sulphur as a consequence of metal-ligand charge transfer. As it is, the peak indicates the electronic transition between p orbital of sulphur and empty 5d orbital of Sn. The appearance of broad shoulder band in the spectra specifically shows the extended conjugation of the complexes (Noureen *et al.*, 2015).

4.9 Anticancer Activity

The dithiocarbamate ligands and a few selected diorganotin complexes; all complexes based on dimethyltin(IV) *bis*(dithiocarbamate) series and two complexes based on dimethyltin(IV)chloride dithiocarbamate series were screened and evaluated against three carcinoma cell lines; lung (A549), prostate (PC-3), and breast (MCF-7). In this study, not all synthesized complexes were examined due to time constraint. The synthesized compounds were screened using MTT cytotoxicity assay. The method on MTT assay was briefly explained in the methodology section.

Cisplatin was used as a positive control. The IC_{50} value for cisplatin against MCF-7 cell line in this study was 9.47 µg/mL. The value is approximately in the accepted range based on the literature value, where the IC_{50} value of cisplatin against MCF-7 were 7.74 µg/mL (Elizabeth *et al.*, 2006), 8.41 µg/mL (Ma *et al.*, 2016), and 23.32 µg/mL (Marciniec *et al.*, 2017). The cytotoxic activity of each sample was expressed as IC_{50} value, which is the concentration of the test sample that causes 50% inhibition of cell growth. The bar chart in **Figure 4.20** and **Figure 4.21** shows the comparison of the IC_{50} value between the ligands and complexes. It can be observed in **Figure 4.21** that **C4** and **C7** display high cytotoxicity activities against all the tested cell line. Specifically, it can be seen that all the diorganotin complexes exhibited better cytotoxicity against the tested human breast cancer cell line (MCF-7) as compared to the ligand itself.

The screening results against human breast cancer cell line (MCF-7) show that **C7** displayed the most active activities among all the complexes with IC_{50} value of 0.4 µg/mL but exhibited lower cytotoxicity than di(4-cyanobenzyl)tin (IV) dithiocarbamates studied by Yin & Xue (2006) which displayed IC_{50} value of 0.0042 µg/mL. This high cytotoxicity of di(4-cyanobenzyl)tin (IV) dithiocarbamates was probably due to the presence of benzyl group that attaches to the Sn atom which increases the lipophilic properties of compound (Yin & Xue, 2006). Nevertheless, **C7** showed better cytotoxicity than cisplatin and

paclitaxel that possess IC_{50} value of 9.47 µg/mL and 5.11 µg/mL, respectively (Fang *et al.*, 2011). Therefore, **C7** was selected to be further studied for encapsulation and drug delivery.

Most of diorganotin dithiocarbamate complexes exhibit better cytotoxicity than the ligand itself as clearly observed in human breast cancer cell line where the IC_{50} value of **L1** ligand is 27.27 µg/mL while its complexes **C1** and **C6** have the IC_{50} value of 0.66 µg/mL and 1.18 µg/mL, respectively. This is contributed by the presence of dimethyltin in the complex that increases the anticancer property as the organotin(IV) toxicity depends on the number and nature of organic moieties. It could also be due to the lipophilic properties of dithiocarbamate ligand which enable the transportation of metal to cellular environment that affect the cytotoxicity activity (Kamaludin *et al.*, 2013).

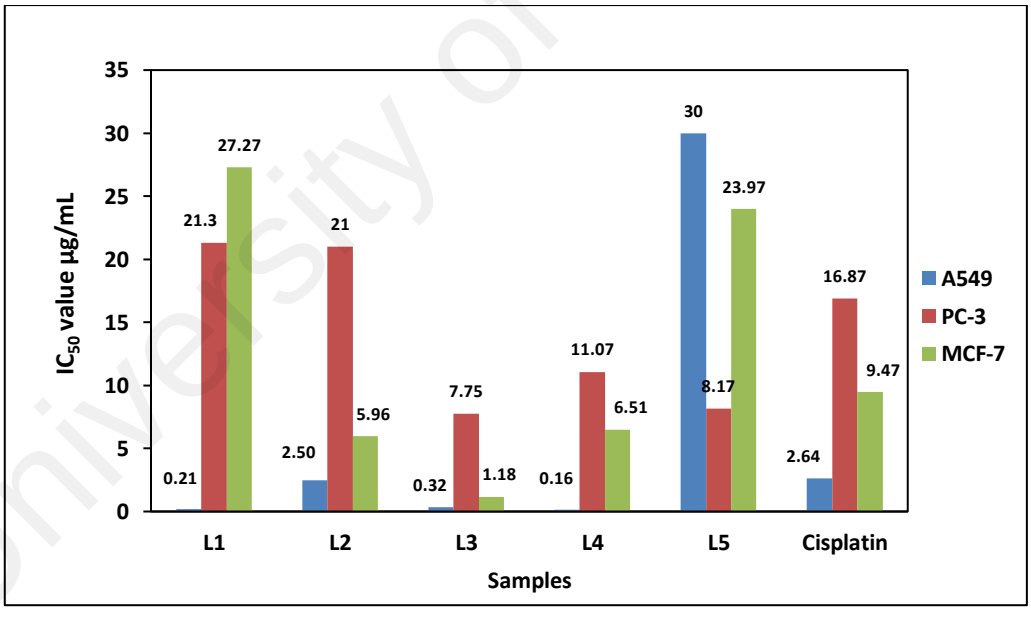

Figure 4.20: Bar chart representation of anticancer activity of dithiocarbamate ligands.

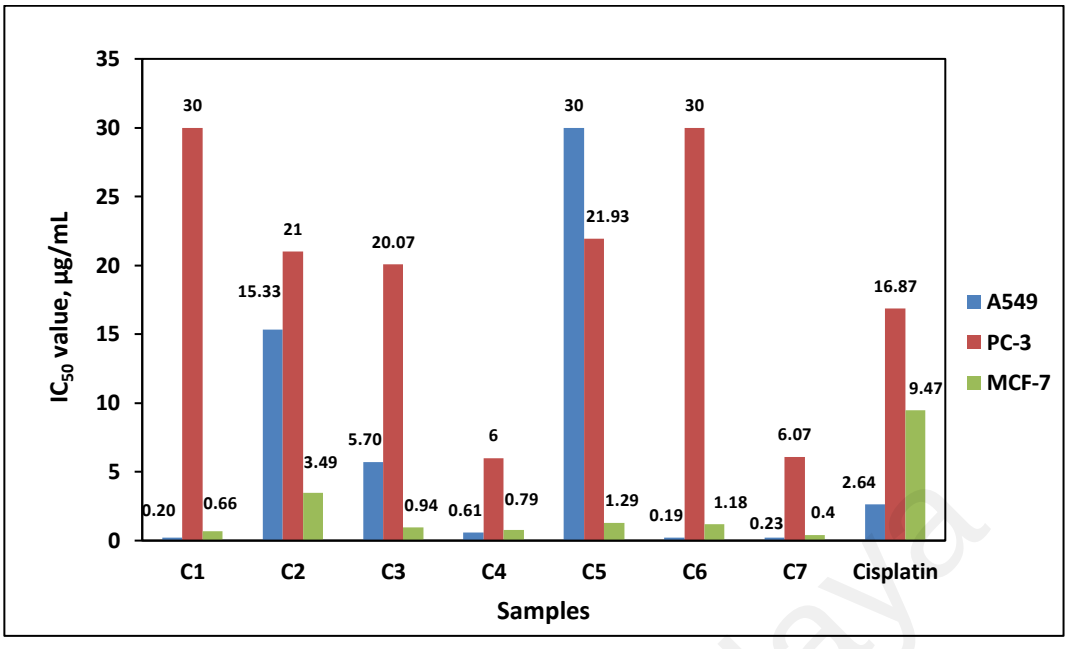

Figure 4.21: Bar chart representation anticancer activity of diorganotin complexes.

4.10 Encapsulation Studies

Dimethyltin(IV)chloride *N,N*-diethyldithiocarbamate (**C7**) was selected to be further analyzed in encapsulation studies as it possesses the highest cytotoxicity activity amongst the studied compound against human breast cancer cell line (MCF-7). Further findings on the encapsulation studies will be discussed in the next section.

4.10.1 Percentage Encapsulation Efficiency and Percentage Drug Loading

From **Table 4.4**, the percentage of encapsulation efficiency (%EE) and the drug loading percentage (%DL) of the dimethyltin(IV)chloride *N,N*-diethyldithiocarbamate (C7) obtained are more than 99% and 88%, respectively. The sample preparations and the calculations of the %EE and %DL were performed in duplicate and the results are reproducible. Numerous factors can affect the encapsulation efficiency of drug such as the size and types of vesicles, the charge on vesicles surface, and the preparation method. One of the factors affecting the high percentage of encapsulation efficiency and drug loading in this formulation studies is the chemical nature of the drug which has poor solubility in water (hydrophobic). Since the drug has low affinity towards an inner and

external aqueous phase, the drug is likely to have a greater affinity towards the hydrophobic region of the vesicles. In this case, the loss of entrapped drug from the vesicles upon extended period of storage could be avoided as they remain entrapped in hydrophobic regions (Kulkarni *et al.*, 1995; Muzzalupo *et al.*, 2017). Thus, it leads to an increase in the percentage of encapsulation efficiency. The high percentage of encapsulation efficiency will result in stronger therapeutic effect and minimised the side effects of the drug (Tavano *et al.*, 2014; Ong *et al.*, 2016). Hydrophilic drugs on the other hand may diffuse in and out of the vesicles membrane. Consequently, the hydrophilic drug will be unable to retain inside the vesicles and results in lower percentage of encapsulation efficiency (Nii & Ishii, 2005).

Table 4.4: Percentage of encapsulation efficiency and drug loading.

Sample	%EE	%DL
Dimethyltin(IV)chloride *N,N*-diethyldithiocarbamate, C7	> 90	88
Paclitaxel-loaded phosphonated calixarene nanovesicles (PCV_{PTX})	90.2	4.1

These observations have been previously reported by Mo *et al.* (2016) where paclitaxel-loaded phosphonated calixarene nanovesicles (PCV_{PTX}) possess high percentage of encapsulation efficiency at 90.2 %. According to Mo *et al.* (2016), another factor affecting the percentage of encapsulation efficiency was the amount ration of drug to nanoparticles used in their work, the molar ration of PCV to PTX is 4:1 (Mo *et al.*, 2016).

Percentage of encapsulation efficiency and drug loading could also be affected by the surface area of thin films formed that consequently affect the hydration process of the vesicles bilayer (Kulkarni *et al.*, 1995). This can be observed in the encapsulation of

doxorubicin-loaded liposomes using different hydration techniques studied by (Amselem *et al.*, 1990).

In addition, the type of solvent used also play an important role in order to achieve high encapsulation efficiency. This can be observed during the preparation of vesicles in this study where the C7 drug is dissolved in organic solvent and the drug still remain entrapped in the hydrophobic bilayer of vesicles throughout hydration phase with phosphate buffer saline (PBS) (Kalepu *et al.*, 2013; Ong *et al.*, 2016) as opposed when using aqueous solvent such as water, salts, and etc.

4.10.2 Particle Size Distribution and Zeta Potential

Particle size distribution and zeta potential were utilized to indicate the colloidal stability of vesicles with the encapsulated drug. The particle size distribution is the key parameter in determining the circulation half-life of vesicles that depends on nature and composition of the vesicles bilayer. Different types of preparation method could also influence the size of vesicles produced; for example, ether/ethanol injection, sonication, and extrusion method will produce vesicle size below 100 nm. Whereas, vesicle size of more than 100 nm to 500 nm are obtained from thin film hydration and freeze-drying method (Batzri & Korn, 1973; Ohsawa *et al.*, 1984). Thus, the thin film hydration method used in this study highly influence the vesicle size obtained in this work. The vesicle size recorded in **Table 4.5** and **Figure 4.22** is 119 ± 9 nm which is smaller than the size of paclitaxel (PTX) loaded with liposomes (DMPC, DMPG, DPPC, and DSPG) that have the size range of 140 nm to 180 nm. Particles with this size range will allow the liposome to extravasate and reach the tumour tissue promptly (Heney *et al.*, 2010). Based on the literature surveys, drug carrier size of below 200 nm will benefit in enhancing permeability and retention (EPR) for extravasation into tumours and more suitable for intravenous injection (Nagayasu *et al.*, 1999; Toy *et al.*, 2014). Since the smallest capillaries in the body are 5–6 μm in diameter, particle size of below 5μm can be easily

distributed into the bloodstream and prevent aggregation of particles that may results in embolism (Singh & Lillard, 2009). The smaller the particle size, the larger the surface area of drug where the increase in the surface area to volume ratio will make the drug more accessible for solvation. Generally, small size particles will allow an efficient uptake of the drugs by a variety of cell types and assist in selective drug accumulation at the target sites (Panyam & Labhasetwar, 2003). In addition, the drug can stay in blood circulation for a longer period of time and can be more easily released from the vesicles thus increasing the bioavailability of the drugs (Dhand *et al.*, 2014; Khadka *et al.*, 2014).

Table 4.5: Analytical data of particle size distribution.

Drugs	Polydispersity Index (PDI)	Size(d.nm)	Zeta potential, mV
C7	0.9 ± 0.1	119 ± 9	-11 ± 1
PTX	0.4 ± 0.1	143 ± 8	-31 ± 4

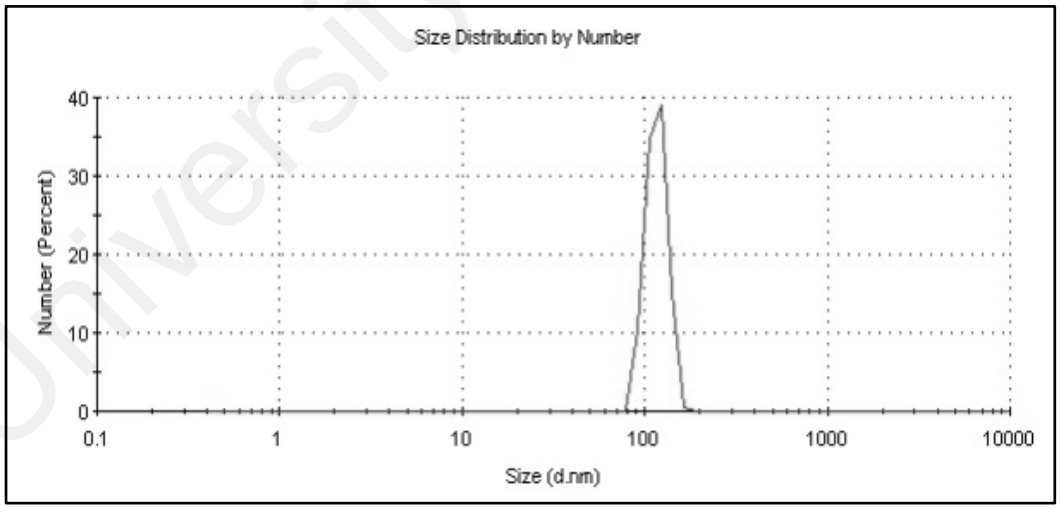

Figure 4.22: Size distribution of C7 by dynamic light scattering (DLS) analysis.

In this study, the polydispersity index (PDI) provides indication on the vesicles stability and its size distributions. The PDI stated in **Table 4.4** is 0.9 ± 0.1 indicates an inhomogeneous and polydisperse particle distribution (Tavano *et al.*, 2014). The result agrees with the shape of particles viewed under FESEM. The shapes of the particles are not a spherical but an oblate and discussed in further details in **Section 4.10.4**. A wider range of PDI indicates a lower stability of particles as it implies the presence of aggregation of nanoparticles (Masarudin *et al.*, 2015). In order to prevent aggregation and to maintain a low PDI value, factors such as type and concentration of surfactants are usually emphasised on. Typically, low value of PDI will be obtained when the concentration of surfactant is high (Sharma *et al.*, 2016).

Zeta potential is a measurement of electrostatic properties of vesicles surface which act as a repulsive energy barrier (Tavano *et al.*, 2014). If the particles suspension has a large negative or positive zeta potential, it indicates a high electric charge on the surface of the drug-loaded nanoparticles. These highly-charged nanoparticles will tend to repel each other by the strong repellent force and preventing the tendency for flocculation (Zhang & Feng, 2006; Laouini *et al.*, 2012). Zhang and Feng (2006) have previously reported that the negatively-charged paclitaxel-loaded polylactide tocopheryl polyethylene glycol succinate (PLA–TPGS) nanoparticles were found stable with average zeta potential value of −30 mV. Based on previously reported literatures, the borderline minimum value of colloidal stability was at ±30 mV. Hence, suspensions with zeta potentials more than ±30 mV are considered stable (Lin *et al.*, 2013). The zeta potential recorded in this work (**Table 4.5)** is −11.1 ± 1 mV showing that the suspension is an unstable colloidal system. It indicates that the particles suspension is not suitable to be stored in colloidal state since the colloidal state formulation results in more stability problem than in the dry form. To overcome this problem, the particles suspension was suggested to be stored in lyophilised state (Mukherjee *et al.*, 2008). Freeze drying method

could be utilized in order to improve the stability of the particles suspension. In this method, the particle suspension undergoes sublimation and desorption process under vacuum to remove water from a frozen sample (Abdelwahed *et al.*, 2006).

4.10.3 Drug Release Studies

There are many factors that affect the drug release including the particle size of vesicles, drug solubility, drug interaction, and drug concentration. **Figure 4.23** shows C7 drug release profile from mixed vesicles carrier. The pH of the release medium was 7.4. Based on the profile, vesicles showed slow release pattern with slight burst effect on day 8 where 21.6% of C7 drug was released. This slight burst effect was due to the drug substance that adsorbed on the vesicles surface or it could be the dispersion of drug near the surface of the nanoparticles (Tarvirdipour *et al.*, 2016). After the burst, it was followed by a stage of slow release amounting to 58% of cumulative C7 drug release percentage from the vesicles within 60 days. Based on the observation, the drug is still being released beyond that period as the C7 drug release is prolonged by the vesicle encapsulation. From the observation, we can assume that the vesicles will shield the C7 drug from being released completely in the biological environment of healthy tissues as concluded by Tiwari and co-worker in the release mechanism of drugs (Tiwari *et al.*, 2012). The release profile pattern of this C7 is comparable to drug release profile of paclitaxel-loaded polylactide tocopheryl polyethylene glycol succinate (PLA–TPGS) nanoparticles where it displayed the initial burst of 22.3% and resulted in 55% of accumulative drug release after 30 days. This indicates that C7-loaded vesicles could give similar performance with paclitaxel-loaded PLA–TPGS nanoparticle based on the drug release profile (Zhang & Feng, 2006).

From the results, we can say that the drug will be able to achieve its stability in blood circulation that allow the drug to be released slowly at the target site. This indicates that the vesicles formulation has fulfils the requirements for an efficient drug delivery system

(Panwar *et al.*, 2010). It shows that the release of C7 drug can be sustained and controlled by encapsulating the drug in vesicles which could improve the pharmacokinetic and pharmacodynamic properties of the drug release (Tavano *et al.*, 2014).

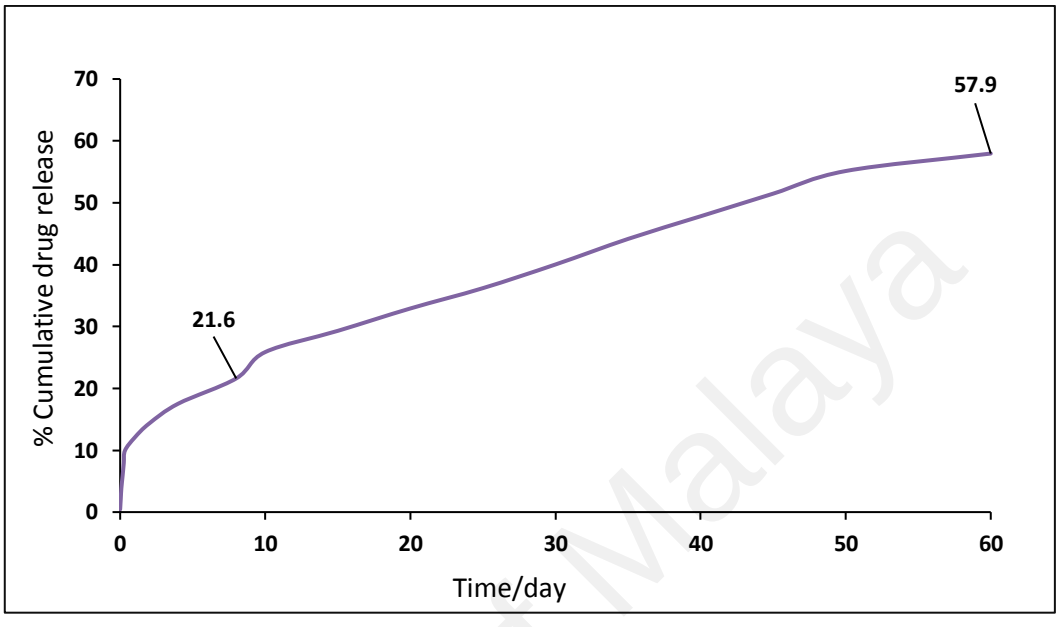

Figure 4.23: *In vitro* C7 release profiles in PBS solution.

4.10.4 Morphological Analysis by FESEM

This FESEM image in **Figure 4.24** shows the average size of drug carrier with an oblate shape. It can be observed with naked eyes that the solution of vesicles containing complex C7 as prepared in **Section 3.5.2** contains large particles size and can be easily filtered. The solution was filtered using a polycarbonate membrane with pore size 0.2 μm. As previously mentioned, the vesicles size in the filtrate is about 119 nm. Collecting and viewing particles in nano range is quite challenging. Therefore, we decided to look at the form of the filtered vesicles. We believe that the shapes of large and small vesicles are the same. As we can see, there are smaller particles in the FESEM image. The shape of drug carriers plays a significant role in delivery process, for example, in particle adhesion, distribution, and cell internalization. Different shapes of drug carriers will give different

circulation time, biodistribution, cellular uptake, and also target site in cancer drug delivery (Liu *et al.*, 2012).

It was found that oblate shape can tumble and rotate, which increase the mobility of the drug carrier towards the blood vessel walls in microcirculation. From previous literatures, drug carriers with oblate shape have better circulation in blood due to its lower uptake by macrophages. Therefore, it can be sustained in blood circulation and as a consequence, increasing their probability to reach the target sites. In addition, this oblate shape plays an important role in controlling endocytosis process by normal and cancer cells (Toy *et al.*, 2014). Besides, it gives small effect by shear and allows effective interaction with the cell surfaces (Truong *et al.*, 2015).

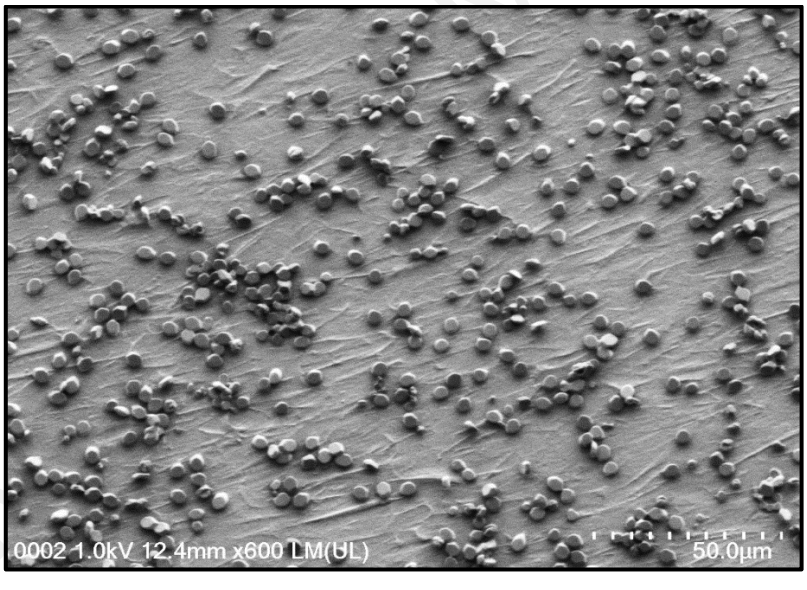

Figure 4.24: FESEM photograph of drug carriers with C7 encapsulated.

CHAPTER 5: CONCLUSIONS

The synthesized complexes were studied by various spectroscopic methods including infrared (IR), ^{1}H-NMR, ^{13}C-NMR, and UV-Vis spectroscopy as well as CHNS elemental analysis. The IR spectra of dithiocarbamate ligands and their diorganotin complexes displayed the presence of common functional groups such as C=N, C-S, Sn-C, and C-H. The ^{1}H-NMR and ^{13}C-NMR spectroscopies identified the environment of the proton and carbon atoms in the ligands and its complexes. Both ^{1}H-NMR and ^{13}C-NMR spectroscopies displayed shifted chemical shift when new signals of methyl group attached to tin atom appeared in the spectrum. This confirms the formation of dithiocarbamate complexes. Meanwhile, the UV-Vis spectroscopies provide the electronic transitions present in the synthesized complexes. Two bands were found; in the ranges 206 nm to 206 nm for dithiocarbamate ligands which assigned to π–π^* transitions and the second band in the ranges 277 nm to 301 nm for ligands coordinated with tin which attributed to n–π^* transitions. In conclusion, ten mixed diorganotin dithiocarbamates complexes were successfully synthesized and characterized.

In general, the diorganotin complexes showed better cytotoxic activity than the dithiocarbamate ligands itself for human breast cancer cell line (MCF-7). However, most of the diorganotin complexes showed poor cytotoxic activity than the ligands in human lung carcinoma cell line (A549) and human prostate cancer cell line (PC-3). Nevertheless, one of the complexes, the dimethyltin(IV)chloride *N,N*-diethyldithiocarbamate (C7) exhibited good cytotoxic activities against all the tested cell lines.

For encapsulation studies, the selected compound; dimethyltin(IV)chloride *N,N*-diethyldithiocarabamate encapsulated in cationic/non-ionic vesicles was successfully prepared and it possessed high encapsulation efficiency with ideal size

distribution, and slow release profile. This study could provide a new innovation in the treatment of breast cancer.

In the future, more parameters can be investigated in the encapsulation studies such as variability concentration of surfactant, variability ratio of surfactant, and application of another technique in drug carrier preparation to further reduce the carrier size and to obtain the optimum PDI value. While taking these variables into account, further studies on this potential drug need to be undertaken. In addition, other prepared diorganotin complexes could be further studied for encapsulation and drug release applications for other cancer cell line such as human prostate cancer and human lung carcinoma since they showed better potential against these two cell lines. The diorganotin complexes could also be screened for other biological activities such as antibacterial and antifungal to further explore their potentials. Besides, the various substituents (ethyl, butyl, and phenyl) that coordinate to tin atom could be explored in order to understand more on the influence of substituents in biological activities and to grow more crystals from the synthesized compounds.

Based on the biological tests results and formulation outcomes, it can be concluded that diorganotin(IV) dithiocarbamate posed a great potential in the pharmaceutical field for breast cancer therapies.

REFERENCES

Abdelwahed, W., Degobert, G., Stainmesse, S., and Fessi, H. (2006). Freeze-drying of nanoparticles: formulation, process and storage considerations. *Advanced Drug Delivery Reviews, 58*(15), 1688-1713.

Abhish, B. J., and Savkare, A. D. (2015). Solid lipid nanoparticles as novel drug delivery system: an overview. *World Journal of Pharmaceutical Research, 4*(3), 352-370.

Abu-El-Halawa, R., and Zabin, S. A. (2017). Removal efficiency of Pb, Cd, Cu and Zn from polluted water using dithiocarbamate ligands. *Journal of Taibah University for Science, 11*(1), 57-65.

Ai, X., Zhong, L., Niu, H., and He, Z. (2014). Thin-film hydration preparation method and stability test of DOX-loaded disulfide-linked polyethylene glycol 5000-lysine-di-tocopherol succinate nanomicelles. *Asian Journal of Pharmaceutical Sciences, 9*(5), 244-250.

Alama, A., Tasso, B., Novelli, F., and Sparatore, F. (2009). Organometallic compounds in oncology: implications of novel organotins as antitumor agents. *Drug Discovery Today, 14*(9-10), 500-508.

Amselem, S., Gabizon, A., and Barenholz, Y. (1990). Optimization and upscaling of doxorubicin-containing liposomes for clinical use. *Journal of Pharmaceutical Science, 79*, 1045-1052.

Arjmand, F., Parveen, S., Tabassum, S., and Pettinari, C. (2014). Organo-tin antitumor compounds: their present status in drug development and future perspectives. *Inorganica Chimica Acta, 423*, 26-37.

Awang, N., Baba, I., M. Yamin, B., Othman, M. S., and Kamaludin, N. F. (2011). Synthesis, characterization and biological activities of organotin (IV) methylcyclohexyldithiocarbamate compounds. *American Journal of Applied Sciences, 8*(4), 310-317.

Awang, N., Mohd Yousof, N. S. A., Baba, I., Rajab, N. F., Hamid, A., M. Yamin, B., and Halim, A. A. (2010). Synthesis and characterization of organotin(IV) N-methyl-N-isopropyldithiocarbamate compounds: X-ray crystal structure of $(CH_3)_2Sn[S_2CN(CH_3)(i\text{-}C_3H_7)]_2$. *World Applied Sciences Journal, 9*(7), 804-810.

Azmin, M. N., Florence, A. T., Handjani-Vila, R. M., Stuart, J. F. B., Vanlerberghe, G., and Whittaker, J. S. (1985). The effect of non-ionic surfactant vesicle (niosome) entrapment on the absorption and distribution of methotrexate in mice. *Journal of Pharmacy and Pharmacology, 37*(4), 237-242.

Baba, I., Muthalib, A. F. A., Aziz, Y. F. A., and Weng, N. S. (2011). New dithiocarbamate compounds from organotin(IV). *Phosphorus, Sulfur, and Silicon and the Related Elements, 186*(6), 1326-1329.

Basirah, A., Hasan, M. F. A., Sidek, N. M., Khairul, W. M., and Ismail, N. (2013). Synthesis, characterization and antimicrobial activity of organotin(IV) complexes featuring bis-2-methoxyethyl dithiocarbamate as ligand. *Journal of Applied Sciences Research, 9*(10), 5562-5567.

Batzri, S., and Korn, E. D. (1973). Single bilayer liposomes prepared without sonication. *Biochimica et Biophysica Acta (BBA) - Biomembranes, 298*(4), 1015-1019.

Berger, N., Sachse, A., Bender, J., Schubert, R., and Brandl, M. (2001). Filter extrusion of liposomes using different devices: comparison of liposome size, encapsulation efficiency, and process characteristics. *International Journal of Pharmaceutics, 223*(1-2), 55-68.

Bergstrom, L. M., and Garamus, V. M. (2012). Structural behaviour of mixed cationic surfactant micelles: a small-angle neutron scattering study. *Journal of Colloid and Interface Science, 381*(1), 89-99.

Blasco, C., Font, G., and Picó, Y. (2004). Determination of dithiocarbamates and metabolites in plants by liquid chromatography–mass spectrometry. *Journal of Chromatography A, 1028*(2), 267-276.

Bruckman, M. A., Czapar, A. E., VanMeter, A., Randolph, L. N., and Steinmetz, N. F. (2016). Tobacco mosaic virus-based protein nanoparticles and nanorods for chemotherapy delivery targeting breast cancer. *Journal of Controlled Release, 231*, 103-113.

Buac, D., Schmitt, S., Ventro, G., Kona, F. R., and Dou, Q. P. (2012). Dithiocarbamate-based coordination compounds as potent proteasome inhibitors in human cancer cells. *Mini-Reviews in Medicinal Chemistry, 12*(12), 1193-1201.

Castrejón-Antúnez, Á. Y., Mendoza-Mendoza, M., Olea-López, D. I., Medrano, F., Tlahuext, H., Guerrero-Álvarez, J., Vargas-Pineda, G., and Godoy-Alcántar, C. (2016). Chlorodiphenyltin(IV) dithiocarbamate complexes as chemodosimeters and host for anions and neutral compounds in solution. *Polyhedron, 111*, 132-142.

Cepeda, V., Fuertes, M. A., Castilla, J., Alonso, C., Quevedo, C., and Perez, J. M. (2007). Biochemical mechanisms of cisplatin cytotoxicity. *Anticancer Agents Medicinal Chemistry, 7*(1), 3-18.

Cevc, G. (2004). Lipid vesicles and other colloids as drug carriers on the skin. *Advanced Drug Delivery Reviews, 56*(5), 675-711.

Coucouvanis, D. (1979). *Progress in inorganic chemistry* (Vol. 26). New York: John Wiley.

D'Souza, S. S., and DeLuca, P. P. (2006). Methods to assess in vitro drug release from injectable polymeric particulate systems. *Pharmaceutical Research, 23*(3), 460-474.

Danoff, E. J., Wang, X., Tung, S. H., Sinkov, N. A., Kemme, A. M., Raghavan, S. R., and English, D. S. (2007). Surfactant vesicles for high-efficiency capture and separation of charged organic solutes. *Langmuir, 23*(17), 8965-8971.

Dhand, C., Prabhakaran, M. P., Beuerman, R. W., Lakshminarayanan, R., Dwivedi, N., and Ramakrishna, S. (2014). Role of size of drug delivery carriers for pulmonary and intravenous administration with emphasis on cancer therapeutics and lung-targeted drug delivery. *Royal Society of Chemistry Advances, 4*(62), 32673-32689.

Dragicevic-Curic, N., Grafe, S., Gitter, B., Winter, S., and Fahr, A. (2010). Surface charged temoporfin-loaded flexible vesicles: in vitro skin penetration studies and stability. *International Journal of Pharmaceutics, 384*(1-2), 100-108.

Dufes, C., Muller, J.-M., Couet, W., Olivier, J.-C., Uchegbu, I. F., and Schätzlein, A. G. (2004). Anticancer drug delivery with transferrin targeted polymeric chitosan vesicles. *Pharmaceutical Research, 21*(1), 101-107.

Ekennia, A. C., Onwudiwe, D. C., Ume, C., and Ebenso, E. E. (2015). Mixed ligand complexes of N-Methyl-N-phenyl dithiocarbamate: Synthesis, characterisation, antifungal activity, and solvent extraction studies of the ligand. *Bioinorganic Chemistry and Applications, 2015*, 913424-913433.

Elizabeth, G., Guadalupe, C., and Teresa, R. (2006). Synthesis, characterization and in vitro cytotoxicity of pentacoordinated tin(IV) complexes derived from aminoalcohols. *Chemical & Pharmaceutical Bulletin, 54*(1), 54-57.

Ezzati Nazhad Dolatabadi, J., Hamishehkar, H., Eskandani, M., and Valizadeh, H. (2014). Formulation, characterization and cytotoxicity studies of alendronate sodium-loaded solid lipid nanoparticles. *Colloids and Surfaces. B, Biointerfaces, 117*, 21-28.

Fadeeva, V. P., Tikhova, V. D., and Nikulicheva, O. N. (2008). Elemental analysis of organic compounds with the use of automated CHNS analyzers. *Journal of Analytical Chemistry, 63*(11), 1094-1106.

Fang, W., Liu, S., and Nie, Y. (2011). Anticancer activity of chamaejasmine: effect on tubulin protein. *Molecules, 16*(8), 6243-6254.

Farina, Y., Othman, A. H., Baba, I., Ng, S. W., and Fun, H.-K. (2002). Organotin dithiocarbamates derived from hydroxylated amines. *Main Group Metal Chemistry, 25*(1-2), 67-72.

Farrugia, L. J. (2012). WinGXandORTEP for windows: an update. *Journal of Applied Crystallography, 45*(4), 849-854.

Ferreira, I. P., de Lima, G. M., Paniago, E. B., Rocha, W. R., Takahashi, J. A., Pinheiro, C. B., and Ardisson, J. D. (2012). Design, structural and spectroscopic elucidation, and the in vitro biological activities of new diorganotin dithiocarbamates. *Europen Journal of Medicinal Chemistry, 58*, 493-503.

Ferreira, I. P., de Lima, G. M., Paniago, E. B., Rocha, W. R., Takahashi, J. A., Pinheiro, C. B., and Ardisson, J. D. (2014). Design, structural and spectroscopic elucidation, and the in vitro biological activities of new triorganotin dithiocarbamates – Part II. *Polyhedron, 79*, 161-169.

Fry, D. W., White, J. C., and Goldman, I. D. (1978). Rapid separation of low molecular weight solutes from liposomes without dilution. *Analytical Biochemistry, 90*(2), 809-815.

Fuentes-Martínez, J. P., Toledo-Martínez, I., Román-Bravo, P., García, P. G. y., Godoy-Alcántar, C., López-Cardoso, M., and Morales-Rojas, H. (2009). Diorganotin(IV) dithiocarbamate complexes as chromogenic sensors of anion binding. *Polyhedron, 28*(18), 3953-3966.

Funato, K., Yoda, R., and Kiwada, H. (1992). Contribution of complement system on destabilization of liposomes composed of hydrogenated egg phosphatidylcholine in rat fresh plasma. *Biochimica et Biophysica Acta, 1103*(2), 198-204.

Geng, T., Zhang, C., Jiang, Y., Ju, H., and Wang, Y. (2017). Synergistic effect of binary mixtures contained newly cationic surfactant: interaction, aggregation behaviors and application properties. *Journal of Molecular Liquids, 232*, 36-44.

Gielen, M., and Tiekink, E. R. T. (2005). *Metallotherapeutic drugs and metal-based diagnostic agents the use of metals in medicine*. Hoboken, N.J.: Wiley.

Harris, J. M., and Chess, R. B. (2003). Effect of pegylation on pharmaceuticals. *Nature Reviews Drug Discovery, 2*(3), 214-221.

Hassan, E. A., and Zayed, S. E. (2014). Dithiocarbamates as precursors in organic chemistry; synthesis and uses. *Phosphorus Sulfur and Silicon and the Related Elements, 189*(3), 300-323.

Heard, P. J. (2005). *Main group dithiocarbamate complexes, ch. 1, progress in inorganic chemistry* (Vol. 53). Hoboken, NJ, USA: John Wiley & Sons, Inc.

Heney, M., Alipour, M., Vergidis, D., Omri, A., Mugabe, C., Th'ng, J., and Suntres, Z. (2010). Effectiveness of liposomal paclitaxel against MCF-7 breast cancer cells. *Canadian Journal of Physiology and Pharmacology, 88*(12), 1172-1180.

Hogarth, G. (2012). Metal-dithiocarbamate complexes: chemistry and biological activity. *Mini-Reviews in Medicinal Chemistry, 12*(12), 1202-1215.

Holeček, J., Nádvorník, M., Handlíř, K., and Lyčka, A. (1986). ^{13}C and ^{119}Sn NMR spectra of di-n-butyltin(IV) compounds. *Journal of Organometallic Chemistry, 315*(3), 299-308.

Honda, M., Komura, M., Kawasaki, Y., Tanaka, T., and Okawara, R. (1968). Infra-red and PMR spectra of some organotin(IV) N,N-dimethyldithiocarbamates. *Journal of Inorganic and Nuclear Chemistry, 30*(12), 3231-3237.

Hsu, K.-H., and Chen, C. (2010). The effect of calibration equations on the uncertainty of UV–Vis spectrophotometric measurements. *Measurement, 43*(10), 1525-1531.

Huang, Y., Chen, J., Chen, X., Gao, J., and Liang, W. (2008). PEGylated synthetic surfactant vesicles (niosomes): novel carriers for oligonucleotides. *Journal of Material Science. Materials in Medicine, 19*(2), 607-614.

Husain, A., Nami, S. A., and Siddiqi, K. S. (2009). Interaction of organotin with piperazine derived self-assembled cylindrical bisdithiocarbamates: spectral and thermal investigations. *Spectrochimica Acta. Part A, Molecular Biomolecular Spectroscopy, 73*(1), 89-95.

Hussain, S., Ali, S., Shahzadi, S., Tahir, M. N., and Shahid, M. (2016). Synthesis, characterization, single crystal XRD and biological screenings of organotin(IV) derivatives with 4-(2-hydroxyethyl)piperazine-1-carbodithioic acid. *Journal of Coordination Chemistry, 69*(4), 687-703.

Hussein, M. A., El-Shorbagi, A.-N., and Khallil, A.-R. (2001). Synthesis and antifungal activity of 3,3'-ethylenebis(5-alkyl-1,3,5-thiadiazine-2-thiones). *Archiv der Pharmazie, 334*(10), 305-308.

Hussen, R. S. D. (2010). *Preparation and evaluation of vesicles based on non-ionic branched chain glycolipids.* (PhD Thesis), Universiti Malaya.

Hussen, R. S. D. (2012). *Niosomes from chain-branched glycolipids for drug delivery. Synthesis, formulation and evaluation.* Germany: Lambert Academic Publishing.

Hussen, R. S. D., and Heidelberg, T. (2016). Drug carriers in cancer therapy: administration, formulation and characterization. *International Journal of Pharma Research & Review, 5*(4), 37-45.

Immordino, M. L., Dosio, F., and Cattel, L. (2006). Stealth liposomes: review of the basic science, rationale, and clinical applications, existing and potential. *International Journal of Nanomedicine, 1*(3), 297-315.

Jain, D., Chaturvedi, A., and Upadhyay, R. K. (2012). Synthesis, properties and spectroscopic characterization of some diorganotin(IV) dithiocarbamates complexes. *Research Journal of Pharmaceutical, Biological and Chemical Sciences, 3*(3), 1311-1318.

Jain, S., Jain, V., and Mahajan, S. C. (2014). Lipid based vesicular drug delivery systems. *Advances in Pharmaceutics, 2014*, 1-12.

Jastrzebski, J. T. B. H., Grove, D. M., Boersma, J., van Koten, G., and Ernsting, J.-M. (1991). 119Sn NMR study of organotin compounds having intramolecular Sn—N coordination. *Magnetic Resonance in Chemistry, 29*(13), S25-S30.

Jayaraju, A., Musthak Ahamad, M., Mallikarjuna Rao, R., and Sreeramulu, J. (2012). Synthesis, characterization and biological evaluation of novel dithiocarbamate metal complexes. *Der Pharma Chemica, 4*(3), 1191-1194.

Jhawat, V. C., Saini, V., Kamboj, S., and Maggon, N. (2013). Transdermal drug delivery systems: Approaches and advancements in drug absorption through skin. *International Journal of Pharmaceutical Sciences Review and Research, 20*(1), 47-56.

Kadu, R., Roy, H., and Singh, V. K. (2015). Diphenyltin(IV) dithiocarbamate macrocyclic scaffolds as potent apoptosis inducers for human cancer HEP 3B and IMR 32 cells: synthesis, spectral characterization, density functional theory study andin vitrocytotoxicity. *Applied Organometallic Chemistry, 29*(11), 746-755.

Kalepu, S., Sunilkumar, K. T., Betha, S., and Mohanvarma, M. (2013). Liposomal drug delivery system - a comprehensive review. *International Journal of Drug Development & Research, 5*(4), 62-75.

Kamaludin, N. F., Awang, N., Baba, I., Hamid, A., and Meng, C. K. (2013). Synthesis, characterization and crystal structure of organotin(IV) *N*-butyl-*N*-phenyldithiocarbamate compounds and their cytotoxicity in human leukemia cell lines. *Pakistan Journal of Biological Sciences, 16*(1), 12-21.

Kayser, O., Lemke, A., and Hernandez-Trejo, N. (2005). The impact of nanobiotechnology on the development of new drug delivery systems. *Current Pharmaceutical Biotechnology, 6*(1), 3-5.

Khadka, P., Ro, J., Kim, H., Kim, I., Kim, J. T., Kim, H., Cho, J. M., Yun, G., and Lee, J. (2014). Pharmaceutical particle technologies: an approach to improve drug solubility, dissolution and bioavailability. *Asian Journal of Pharmaceutical Sciences, 9*(6), 304-316.

Khan, H. N., Ali, S., Shahzadi, S., Sharma, S. K., and Qanungo, K. (2010). Synthesis, spectroscopy, semiempirical, phytotoxicity, antibacterial, antifungal, and cytotoxicity of diorganotin(IV) complex derived from $Bu_2Sn(Acac)_2$ and 4-methyl-1-piperidinecarbodithioic acid. *Russian Journal of Coordination Chemistry, 36*(4), 310-316.

Khan, N., Farina, Y., Mun, L. K., Rajab, N. F., and Awang, N. (2015). Syntheses, characterization, X-ray diffraction studies and in vitro antitumor activities of diorganotin(IV) derivatives of bis(p-substituted-N-methylbenzylaminedithiocarbamates). *Polyhedron, 85*, 754-760.

Khan, S., Nami, S. A. A., and Siddiqi, K. S. (2008). Mononuclear indolyldithiocarbamates of $SnCl_4$ and R_2SnCl_2: spectroscopic, thermal characterizations and cytotoxicity assays in vitro. *Journal of Organometallic Chemistry, 693*(6), 1049-1057.

Kim, Y. I., Fluckiger, L., Hoffman, M., Lartaud-Idjouadiene, I., Atkinson, J., and Maincent, P. (1997). The antihypertensive effect of orally administered nifedipine-loaded nanoparticles in spontaneously hypertensive rats. *The British Journal of Pharmacology, 120*(3), 399-404.

Kubik, T., Bogunia-Kubik, K., and Sugisaka, M. (2005). Nanotechnology on duty in medical applications. *Current Pharmaceutical Biotechnology, 6*(1), 17-33.

Kulkarni, S. B., Betageri, G. V., and Singh, M. (1995). Factors affecting microencapsulation of drugs in liposomes. *Journal of Microencapsulation, 12*(3), 229-246.

Lainez, A., del Burgo, P., Junquera, E., and Aicart, E. (2004). Mixed micelles formed byn-octyl-β-d-glucopyranoside and tetradecyltrimethylammonium bromide in aqueous media. *Langmuir, 20*(14), 5745-5752.

Langer, R. (1983). Implantable controlled release systems. *Pharmacology & Therapeutics, 21*(1), 35-51.

Laouini, A., Jaafar-Maalej, C., Limayem-Blouza, I., Sfar, S., Charcosset, C., and Fessi, H. (2012). Preparation, characterization and applications of liposomes: state of the art. *Journal of Colloid Science and Biotechnology, 1*, 147–168.

Lee, S. M., Sim, K. S., and Lo, K. M. (2015). Synthesis, characterization and biological studies of diorganotin(IV) complexes with tris[(hydroxymethyl)aminomethane] schiff bases. *Inorganica Chimica Acta, 429*, 195-208.

Li, W., Luo, T., Yang, Y., Tan, X., and Liu, L. (2015). Formation of controllable hydrophilic/hydrophobic drug delivery systems by electrospinning of vesicles. *Langmuir, 31*(18), 5141-5146.

Lim, S. H., Low, Y. Y., Sinniah, S. K., Yong, K. T., Sim, K. S., and Kam, T. S. (2014). Macroline, akuammiline, sarpagine, and ajmaline alkaloids from Alstonia macrophylla. *Phytochemistry, 98*, 204-215.

Lin, T., Fang, Q., Peng, D., Huang, X., Zhu, T., Luo, Q., Zhou, K., and Chen, W. (2013). PEGylated non-ionic surfactant vesicles as drug delivery systems for gambogenic acid. *Drug Delivery, 20*(7), 277-284.

Liu, Y., Tan, J., Thomas, A., Ou-Yang, D., and Muzykantov, V. R. (2012). The shape of things to come: importance of design in nanotechnology for drug delivery. *Therapeutic Delivery, 3*(2), 181-194.

Ma, J., Wang, Q., Yang, X., Hao, W., Huang, Z., Zhang, J., Wang, X., and Wang, P. G. (2016). Glycosylated platinum(iv) prodrugs demonstrated significant therapeutic efficacy in cancer cells and minimized side-effects. *Dalton Trans, 45*(29), 11830-11838.

Macomber, R. S. (1991). Proton-carbon chemical shift correlations. *Journal of Chemical Education, 68*(4), 284-285.

Manohar, A., Karpagavel, K., and Arasu, p. T. (2013). Characterization studies on 4,4'-bipyridine and cadmium dithiocarbamates involved dimeric complexes and valence bond parameter calculations on some cadmium dithiocarbamate complexes. *International Journal of ChemTech Research, 5*(4), 1486-1494.

Manosroi, A., Ruksiriwanich, W., Abe, M., Sakai, H., Aburai, K., Manosroi, W., and Manosroi, J. (2012). Physico-chemical properties of cationic niosomes loaded with fraction of rice (oryza sativa) bran extract. *Journal of Nanoscience and Nanotechnology, 12*(9), 7339-7345.

Marciniec, K., Pawelczak, B., Latocha, M., Skrzypek, L., Maciazek-Jurczyk, M., and Boryczka, S. (2017). Synthesis, anti-breast cancer activity, and molecular docking

study of a new group of acetylenic quinolinesulfonamide derivatives. *Molecules, 22*(2), 1-19.

Masarudin, M. J., Cutts, S. M., Evison, B. J., Phillips, D. R., and Pigram, P. J. (2015). Factors determining the stability, size distribution, and cellular accumulation of small, monodisperse chitosan nanoparticles as candidate vectors for anticancer drug delivery: application to the passive encapsulation of [(14)C]-doxorubicin. *Nanotechnology, Science and Application, 8*, 67-80.

Mo, J., Eggers, P. K., Yuan, Z. X., Raston, C. L., and Lim, L. Y. (2016). Paclitaxel-loaded phosphonated calixarene nanovesicles as a modular drug delivery platform. *Scientific Reports, 6*, 23489-23501.

Moghassemi, S., and Hadjizadeh, A. (2014). Nano-niosomes as nanoscale drug delivery systems: an illustrated review. *Journal of Controlled Release, 185*, 22-36.

Mohamad, R., Awang, N., Kamaludin, N. F., and Abu Bakar, N. F. (2016). Synthesis, characterisation and antibacterial activity of new diorganotin(IV) bis(2-methoxyethyl)dithiocarbamate complexes. *Research Journal of Pharmaceutical, Biological and Chemical Sciences, 7*(5), 1269-1274.

Mohamad, R., Awang, N., Kamaludin, N. F., Jotani, M. M., and Tiekink, E. R. (2017). Di-n-butyl-bis-[N-(2-meth-oxy-eth-yl)-N-methyl-dithio-carbamato-kappa(2)S,S']tin(IV): crystal structure and Hirshfeld surface analysis. *Acta Crystallographica Section E, Crystallographic Communications, 73*(Pt 2), 260-265.

Mukherjee, B., Santra, K., Pattnaik, G., and Ghosh, S. (2008). Preparation, characterization and in-vitro evaluation of sustained release protein-loaded nanoparticles based on biodegradable polymers *International Journal of Nanomedicine, 3*(4), 487-496.

Muthalib, A. F. A., Baba, I., Farina, Y., and Samsudin, M. W. (2011). Synthesis and characterization of diphenyltin (IV) dithiocarbamate compounds. *Malaysian Journal of Analytical Sciences, 15*(1), 106-112.

Muzzalupo, R., Perez, L., Pinazo, A., and Tavano, L. (2017). Pharmaceutical versatility of cationic niosomes derived from amino acid-based surfactants: skin penetration behavior and controlled drug release. *International Journal of Pharmaceutics, 529*(1-2), 245-252.

Nagayasu, A., Uchiyama, K., and Kiwada, H. (1999). The size of liposomes: a factor which affects their targeting efficiency to tumors and therapeutic activity of liposomal antitumor drugs. *Advanced Drug Delivery Reviews, 40*(1-2), 75-87.

Nath, M. (2008). Toxicity and the cardiovascular activity of organotin compounds: a review. *Applied Organometallic Chemistry, 22*(10), 598-612.

Negm, N. A., and Sabagh, A. M. E. (2011). Interaction between cationic and conventional nonionic surfactants in the mixed micelle and monolayer formed in aqueous medium. *Química Nova, 34*, 1007-1013.

Nii, T., and Ishii, F. (2005). Encapsulation efficiency of water-soluble and insoluble drugs in liposomes prepared by the microencapsulation vesicle method. *International Journal of Pharmaceutics, 298*(1), 198-205.

Noureen, S., Sirajuddin, M., Ali, S., Shaheen, F., and Tahir, M. N. (2015). Synthesis, structural elucidation and DNA binding study of fluorine substituted organotin(IV) dithiocarbamates. *Polyhedron, 102*, 750-758.

Ohsawa, T., Miura, H., and Harada, K. (1984). A novel method for preparing liposome with a high capacity to encapsulate proteinous drugs: freeze-drying method. *Chemical & Pharmaceutical Bulletin (Tokyo), 32*(6), 2442-2445.

Olson, F., Hunt, C. A., Szoka, F. C., Vail, W. J., and Papahadjopoulos, D. (1979). Preparation of liposomes of defined size distribution by extrusion through polycarbonate membranes. *Biochimica et Biophysica Acta (BBA) - Biomembranes, 557*(1), 9-23.

Ong, S. G., Ming, L. C., Lee, K. S., and Yuen, K. H. (2016). Influence of the encapsulation efficiency and size of liposome on the oral bioavailability of griseofulvin-loaded liposomes. *Pharmaceutics, 8*(3), 25-41.

Onwudiwe, D. C., and Ajibade, P. A. (2010). Synthesis and characterization of metal complexes of N-alkyl-N-phenyl dithiocarbamates. *Polyhedron, 29*(5), 1431-1436.

Padamwar, M. N., and Pokharkar, V. B. (2006). Development of vitamin loaded topical liposomal formulation using factorial design approach: drug deposition and stability. *International Journal of Pharmaceutics, 320*(1-2), 37-44.

Panwar, P., Pandey, B., Lakhera, P. C., and Singh, K. P. (2010). Preparation, characterization, and in vitro release study of albendazole-encapsulated nanosize liposomes. *International Journal of Nanomedicine, 5*, 101-108.

Panyam, J., and Labhasetwar, V. (2003). Biodegradable nanoparticles for drug and gene delivery to cells and tissue. *Advanced Drug Delivery Reviews, 55*(3), 329-347.

Papadimitriou, S., and Bikiaris, D. (2009). Novel self-assembled core-shell nanoparticles based on crystalline amorphous moieties of aliphatic copolyesters for efficient controlled drug release. *Journal of Controlled Release, 138*(2), 177-184.

Perrie, Y., Kastner, E., Kaur, R., Wilkinson, A., and Ingham, A. J. (2013). A case-study investigating the physicochemical characteristics that dictate the function of a liposomal adjuvant. *Human Vaccine and Immunotherapeutics, 9*(6), 1374-1381.

Popovska, O., Simonovska, J., Kavrakovski, Z., and Rafajlovska, V. (2013). An Overview: Methods for preparation and characterization of liposomes as drug delivery systems. *International Journal of Pharmaceutical and Phytopharmacological Research, 3*(2), 13-20.

Puri, A., Loomis, K., Smith, B., Lee, J. H., Yavlovich, A., Heldman, E., and Blumenthal, R. (2009). Lipid-based nanoparticles as pharmaceutical drug carriers: from concepts to clinic. *Critical Reviews in Therapeutic Drug Carrier Systems, 26*(6), 523-580.

Qureshi, Q.-u.-A. H., Nadhman, A., Sirajuddin, M., Shahnaz, G., Ali, S., Shah, A., and Yasinzai, M. M. (2014). Organotin(IV) complexes of carboxylate derivative as potential chemotherapeutic agents against leishmania. *Inorganica Chimica Acta, 423*, 220-228.

Remesh, A. (2012). Toxicities of anticancer drugs and its management. *International Journal of Basic & Clinical Pharmacology, 1*(1), 2-12.

Safari, M., Yousefi, M., Jenkins, H. A., Torbati, M. B., and Amanzadeh, A. (2013). Synthesis, spectroscopic characterization, X-ray structure, and in vitro antitumor activities of new triorganotin(IV) complexes with sulfur donor ligand. *Medicinal Chemistry Research, 22*(12), 5730-5738.

Sağlık, B. N., Özkay, Y., Demir Özkay, Ü., and Karaca Gençer, H. (2014). Synthesis and biological evaluation of some novel dithiocarbamate derivatives. *Journal of Chemistry, 2014*, 1-9.

Sainorudin, M. H., Sidek, N. M., Ismail, N., Rozaini, M. Z. H., Harun, N. A., Anuar, T. N. S. T., Azmi, A. A. A. R., and Yusoff, F. (2015). Synthesis, characterization and biological activity of organotin(IV) complexes featuring di-2-ethylhexyldithiocarbamate and N-methylbutyldithiocarbamate as ligands. *Journal of Chemical Sciences, 2*(1), 10-18.

Saritha, A. (2015). Formulation and evaluation of cationic niosomes of 5-fluoro uracil. *Indo American Journal of Pharmaceutical Science, 2*(3), 746-750.

Shaheen, F., Zia-ur-Rehman, Ali, S., and Meetsma, A. (2012). Structural properties and antibacterial potency of new supramolecular organotin(IV) dithiocarboxylates. *Polyhedron, 31*(1), 697-703.

Shahzadi, S., and Ali, S. (2008). Structural chemistry of organotin(IV) complexes. *Journal of the Iranian Chemical Society, 5*(1), 16-28.

Shang, X., Cui, J., Wu, J., Pombeiro, A. J., and Li, Q. (2008). Polynuclear diorganotin(IV) complexes with arylhydroxamates: syntheses, structures and in vitro cytotoxic activities. *Journal of Inorganic Biochemistry, 102*(4), 901-909.

Sharma, N., Madan, P., and Lin, S. (2016). Effect of process and formulation variables on the preparation of parenteral paclitaxel-loaded biodegradable polymeric nanoparticles: a co-surfactant study. *Asian Journal of Pharmaceutical Sciences, 11*(3), 404-416.

Sheldrick, G. M. (2008). A short history of SHELX. *Acta Crystallographica. Section A, Foundations of Crystallography, 64*(Pt 1), 112-122.

Sheldrick, G. M. (2015). Crystal structure refinement with SHELXL. *Acta Crystallographica. Section C, Structural Chemistry, 71*(Pt 1), 3-8.

Singh, N., and Bhattacharya, S. (2012). Synthesis and characterization of some triorgano, diorgano, monoorganotin and a triorganolead heteroaromatic dithiocarbamate complexes. *Journal of Organometallic Chemistry, 700*, 69-77.

Singh, R., Ajagbe, M., Bhamidipati, S., Ahmad, Z., and Ahmad, I. (2005). A rapid isocratic high-performance liquid chromatography method for determination of cholesterol and 1,2-dioleoyl-sn-glycero-3-phosphocholine in liposome-based drug formulations. *Journal of Chromatography A, 1073*(1-2), 347-353.

Singh, R., and Kaushik, N. K. (2008). Spectral and thermal studies with anti-fungal aspects of some organotin(IV) complexes with nitrogen and sulphur donor ligands derived from 2-phenylethylamine. *Spectrochimica Acta Part A-Molecular and Biomolecular Spectroscopy, 71*(2), 669-675.

Singh, R., and Lillard, J. W., Jr. (2009). Nanoparticle-based targeted drug delivery. *Experimental and Molecular Pathology, 86*(3), 215-223.

Sirajuddin, M., Ali, S., Mckee, V., Sohail, M., and Pasha, H. (2014). Potentially bioactive organotin(IV) compounds: Synthesis, characterization, in vitro bioactivities and interaction with SS-DNA. *European Journal of Medicinal Chemistry, 84*, 343-363.

Srikanth, K., Rama Mohan Gupta, V., Raj Manvi, S., and Devanna, N. (2012). Particulate carrier systems : a review. *International Research Journal of Pharmacy, 3*(11), 22-26.

Sun, T., Yan, H., Liu, G., Hao, J., Su, J., Li, S., Xing, P., and Hao, A. (2012). Strategy of directly employing paclitaxel to construct vesicles. *Journal of Physical Chemistry B, 116*(50), 14628-14636.

Szoka, F., Jr., and Papahadjopoulos, D. (1980). Comparative properties and methods of preparation of lipid vesicles (liposomes). *Annual Review of Biophysics and Bioengineering, 9*, 467-508.

Talegaonkar, S., Mishra, P. R., Khar, R. K., and Biju, S. S. (2006). Vesicular systems: an overview. *Indian Journal of Pharmaceutical Sciences, 68*(2), 141-153.

Tarvirdipour, S., Vasheghani-Farahani, E., Soleimani, M., and Bardania, H. (2016). Functionalized magnetic dextran-spermine nanocarriers for targeted delivery of doxorubicin to breast cancer cells. *International Journal of Pharmaceutics, 501*(1-2), 331-341.

Tavano, L., Pinazo, A., Abo-Riya, M., Infante, M. R., Manresa, M. A., Muzzalupo, R., and Perez, L. (2014). Cationic vesicles based on biocompatible diacyl glycerol-arginine surfactants: physicochemical properties, antimicrobial activity, encapsulation efficiency and drug release. *Colloids and Surfaces. B, Biointerfaces, 120*, 160-167.

Tian, L., Sun, Y., Li, H., Zheng, X., Cheng, Y., Liu, X., and Qian, B. (2005). Synthesis, characterization and biological activity of triorganotin 2-phenyl-1,2,3-triazole-4-carboxylates. *Journal of Inorganic Biochemistry, 99*(8), 1646-1652.

Tiekink, E. R. T. (2008). Tin dithiocarbamates: applications and structures. *Applied Organometallic Chemistry, 22*(9), 533-550.

Tiwari, G., Tiwari, R., Sriwastawa, B., Bhati, L., Pandey, S., Pandey, P., and Bannerjee, S. K. (2012). Drug delivery systems: an updated review. *International Journal of Pharmaceutical Investigation, 2*(1), 2-11.

Tokuyama, R., Takahashi, Y., Tomita, Y., Tsubouchi, M., Yoshida, T., Iwasaki, N., Kado, N., Okezaki, E., and Nagata, O. (2001). Structure-activity relationship (SAR) studies on oxazolidinone antibacterial agents. 2. Relationship between lipophilicity and antibacterial activity in 5-thiocarbonyl oxazolidinones. *Chemical & Pharmaceutical Bulletin, 49*(4), 353-360.

Toy, R., Peiris, P. M., Ghaghada, K. B., and Karathanasis, E. (2014). Shaping cancer nanomedicine: the effect of particle shape on the in vivo journey of nanoparticles. *Nanomedicine (Lond), 9*(1), 121-134.

Truong, N. P., Whittaker, M. R., Mak, C. W., and Davis, T. P. (2015). The importance of nanoparticle shape in cancer drug delivery. *Expert Opinion Drug Delivery, 12*(1), 129-142.

Urgut, O. S., Ozturk, I. I., Banti, C. N., Kourkoumelis, N., Manoli, M., Tasiopoulos, A. J., and Hadjikakou, S. K. (2016). New antimony(III) halide complexes with dithiocarbamate ligands derived from thiuram degradation: the effect of the molecule's close contacts on in vitro cytotoxic activity. *Materials Science & Engineering C-Materials for Biological Applications, 58*, 396-408.

Van Gaal, H. L. M., Diesveld, J. W., Pijpers, F. W., and Van der Linden, J. G. M. (1979). Carbon-13 NMR spectra of dithiocarbamates. Chemical shifts, carbon-nitrogen stretching vibration frequencies and .pi.-bonding in the NCS_2 fragment. *Inorganic Chemistry, 18*(11), 3251-3260.

Verma, P., Thakur, A. S., Deshmukh, K., Jha, A. K., and Verma, S. (2010). Routes of drug administration. *International Journal of Pharmaceutical Studies and Research, 1*(1), 54-59.

Xiong, R. G., Zuo, J. L., and You, X. Z. (1997). A novel dimeric zinc complex: bis{μ-[(dimercaptomethylene)propanedinitrilato-S,S']}tetrakis(4-methylpyridine)dizinc(II)-chloroform. *Inorganic Chemistry, 36*(11), 2472-2474.

Yamaguchi, A., K.Tomiyama, Y.Sayama, T.Kuriyama, H.Nakashima, Y.Matsuda, and Y.Arakawa. (2007). Mechanism on the cell death of T-lymphocytes induced by organotin in vitro. *Trace Nutrients Research, 24*, 90-97.

Yassin, A. E. B., Anwer, M. K., Mowafy, H. A., El-Bagory, I. M., Bayomi, M. A., and Alsarra, I. A. (2010). Optimization of 5-flurouracil solid-lipid nanoparticles: a preliminary study to treat colon cancer. *International Journal of Medical Sciences, 7*(6), 398-408.

Yin, H.-D., and Xue, S.-C. (2005). Crystallographic report: di(o-chlorobenzyl)tin(IV) bis(N-methylpiperazinyldithiocarbamate). *Applied Organometallic Chemistry, 19*(1), 194-195.

Yin, H. D., and Xue, S. C. (2006). Synthesis and characterization of organotin complexes with dithiocarbamates and crystal structures of $(4\text{-}NCC_6H_4CH_2)_2Sn(S_2CNEt_2)_2$ and $(2\text{-}ClC_6H_4CH_2)_2\ Sn(Cl)S_2CNBz_2$. *Applied Organometallic Chemistry, 20*(4), 283-289.

Zhang, J. R., Jian, F. F., Lu, L. D., Yang, X. J., and Wang, X. (2001). Structure and characterization of tris(4-morpholinedithiocarbamato-S,S ')cobalt(center dot)-acetonitrile solvate complex: [$Co(S_2CNC_4H_8O)(3)$]center dot CH_3CN. *Journal of Chemical Crystallography, 31*(5), 251-254.

Zhang, L., Cao, D. Y., Wang, J., Xiang, B., Dun, J. N., Fang, Y., and Xue, G. Q. (2013). PEG-coated irinotecan cationic liposomes improve the therapeutic efficacy of breast cancer in animals. *European Review Medical Pharmacological Sciences, 17*(24), 3347-3361.

Zhang, Z., and Feng, S. S. (2006). The drug encapsulation efficiency, in vitro drug release, cellular uptake and cytotoxicity of paclitaxel-loaded poly(lactide)-tocopheryl polyethylene glycol succinate nanoparticles. *Biomaterials, 27*(21), 4025-4033.

Zhao, S., Minh, L. V., Li, N., Garamus, V. M., Handge, U. A., Liu, J., Zhang, R., Willumeit-Romer, R., and Zou, A. (2016). Doxorubicin hydrochloride-oleic acid conjugate loaded nanostructured lipid carriers for tumor specific drug release. *Colloids and Surfaces. B, Biointerfaces, 145*, 95-103.

Zia ur, R., Muhammad, N., Ali, S., Butler, I. S., and Meetsma, A. (2011). Synthesis, spectroscopic properties, X-ray single crystal analysis and antimicrobial activities of organotin(IV) 4-(4-methoxyphenyl)piperazine-1-carbodithioates. *Inorganica Chimica Acta, 376*(1), 381-388.

Zia ur, R., Muhammad, N., Shuja, S., Ali, S., Butler, I. S., Meetsma, A., and Khan, M. (2009). New dimeric, trimeric and supramolecular organotin(IV) dithiocarboxylates: Synthesis, structural characterization and biocidal activities. *Polyhedron, 28*(16), 3439-3448.

LIST OF PUBLICATIONS AND PAPERS PRESENTED

Zaldi, N. B., Hussen, R. S. D., Lee, S. M., Halcovitch, N. R., Jotani, M. M., and Tiekink, E. R. T. (2017). Secondary bonding in di-methyl-bis-(morpholine-4-carbodi-thio-ato-kappa^{2}S,S')tin(IV): crystal structure and Hirshfeld surface analysis. *Acta Crystallographica Section E, Crystallographic Communications, 73*(Pt 6), 842-848.